![Chalmers University of Technology logo](CHALMERS UNIVERSITY OF TECHNOLOGY)
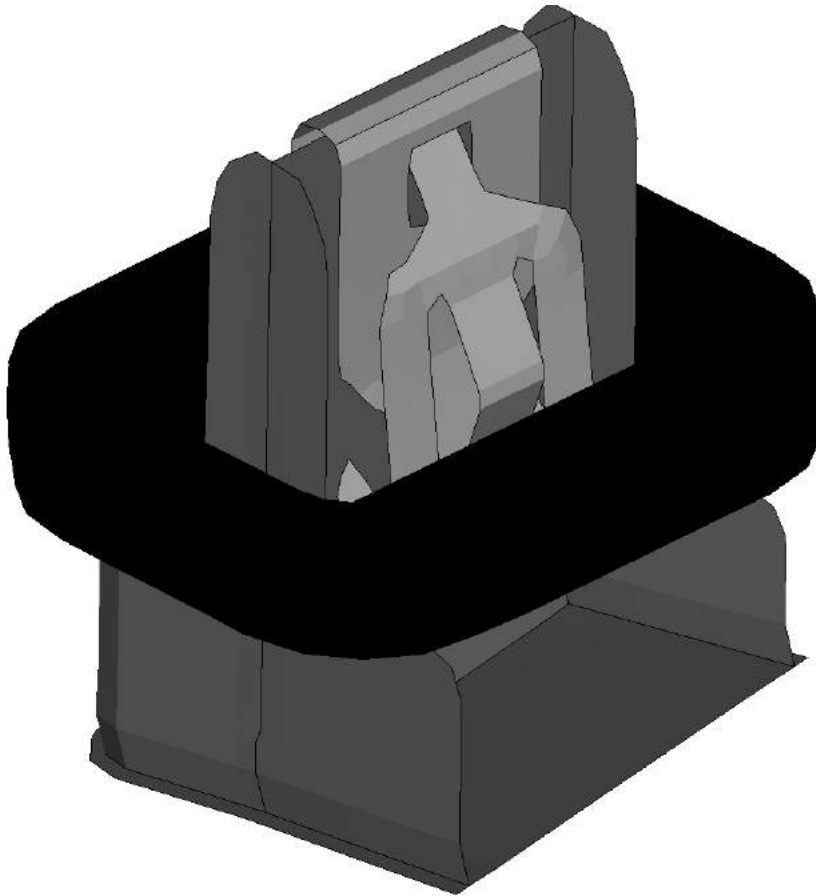
Clip joint modeling

Master's thesis in Applied Mechanics

SEBASTIAN STÅHL

MASTER'S THESIS IN APPLIED MECHANICS

Clip joint modeling

SEBASTIAN STÅHL

Department of Applied mechanics
Division of Material & Computational Mechanics
CHALMERS UNIVERSITY OF TECHNOLOGY

Göteborg, Sweden 2017

Cover:
Picture of the clip joint simulation model.

Clip joint modeling
Master's thesis in Applied Mechanics
SEBASTIAN STÅHL
Department of Applied mechanics
Division of Material & Computational Mechanics
Chalmers University of Technology

ABSTRACT

In the automotive industry many parts are connected with different types of clips. One of them is studied in this Master Thesis. The studied clip is of metal and used to connect plastic parts to each other in the interior of the cars. The aim is to find the mechanical properties of this clip joint at room temperature and $80°C$ and to implement in a simple connector element representing the clip joint.

The properties in the clip connection are determined by use of a combination of component tests and simulations. The tests are performed by fastening one part in the clip connection and applying a displacement at the other part and measuring the force to get a force vs displacement relation. In the finite element simulations are the same loading case used. In the numerical simulations is also a sensitivity analysis performed to investigate what parameters affects the properties of the clip joint the most.

The study gives linear stiffnesses perpendicular to the hole and around all axes. The frictional force when sliding along the hole occurs is determined. The forces needed to assemble and dis-assemble the clip joint are also determined. All these properties are determined both for room temperature and for $80°C$. The determined properties are only valid until a specific displacement when the plastic parts come in contact. From the sensitivity study is concluded that the most important parameters are the hole size and thickness of the clip.

The determined properties make it possible to include a more realistic behavior of the clip joint in simulations with clips. It is possible because the representation in the connector element still is simple but more realistic and prevents the number of degrees of freedom to increase drastically.

Clip förband modelering
Examensarbete i Tillämpad mekanik
SEBASTIAN STÅHL
Institutionen för Tillämpad mekanik
Avdelningen för Material- och beräkningsmekanik
Chalmers Tekniska Högskola

Sammanfattning

I fordonsindustrin är många delar monterade med olika typer av clips. Ett av dessa clip är studerade i det här examensarbete. Det granskade clipet är gjort i metall och används för att montera ihop plastinteriörer i bilar. Målet med studien är att hitta egenskaperna av clipset vid både rumstemperatur och vid $80°C$. De mekaniska egenskaper är sedan implementerade i ett enkelt element kallat connector element som kan representera clipet.

Egenskaperna av clipet är framtagna genom både fysiska tester och numeriska simuleringar. Testerna är gjorda genom att ena delen är fastspänd och sedan är en förskjutning applicerad på den andra delen av clipet. Vid den applicerade förskjutningen är kraften uppmätt för att fastställa relationen mellan kraft och förskjutning. Samma last fall på clipet är analyserat finita element simuleringarna. I simuleringarna är också en känslighetsanalys gjord för att avgöra vilka parametrar som mest påverkar clipets egenskaper.

Studien ger linjära styvheter vinkelrätt mot hålet och runt alla koordinataxlar. Kraften som krävs för glidning längs hålet är också framtagen. I montering och demontering krävs olika krafter som är beräknade i arbetet. Alla egenskaper är utvärderade för både rumstemperatur och för $80°C$. Alla egenskaper gäller enbart tills plastdelarna kommer i kontakt. Från känslighetsanalysen konstaterades att de viktigaste parametrarna för clipets egenskaper är storleken av hålet och tjockleken på clipet.

De framtagna egenskaperna gör att det är möjligt att ha med ett mer realistisk beteende av clipen i simuleringar. Detta är möjligt eftersom att det enkla connector elementet representerar clipet realistiskt utan att avsevärt öka antalet frihetsgrader.

Contents

NOTATIONS

$\boldsymbol{C}$	Damping matrix	Ns/mm and $Nmms/rad$
$\boldsymbol{E}$	Young's modulus	MPa
F_N	Normal force	N
F_a	Applied force	N
F_f	Friction force	N
F_t	Tangential force	N
F_{ass}	Assembly force	N
F_{dis}	Dis-assembly force	N
G	Shear modulus	MPa
$\boldsymbol{I}$	Internal force vector	N and Nmm
$\boldsymbol{K}$	Stiffness matrix	N/mm and Nmm/rad
L_e	Characteristic element length	mm
$\boldsymbol{M}$	Mass matrix	kg and $kgmm^2$
M_a	Applied torque	Nmm
$\boldsymbol{P}$	Constraint matrix	$-$
ΔT	Temperature change from stress free state	$^\circ C$
c	Wave speed in material	mm/s
$d\phi$	Rotation	rad
dy	Displacement	mm
$\boldsymbol{f}$	External force vector	N and Nmm
k_ϕ	Rotational stiffness	Nmm/rad
k_t	Translational stiffness	N/mm
k_y	Stiffness in Y	N/mm
$k_{\phi y}$	Rotational stiffness around Y	Nmm/rad
$k_{\phi z}$	Rotational stiffness around Z	Nmm/rad
$\boldsymbol{q}$	Prescribed displacements	mm
$\boldsymbol{u}$	Displacement and rotation tensor	mm
$\boldsymbol{\Delta\epsilon_{pl}}$	Plastic strain increment	$-$
α	Thermal expansion coefficient	$1/^\circ C$
$\boldsymbol{\epsilon_e}$	Elastic strain tensor	$-$
$\boldsymbol{\epsilon_p}$	Plastic strain tensor	$-$
$\boldsymbol{\sigma_{dev}}$	Deviatoric stress tensor	MPa
$\boldsymbol{\sigma_{vol}}$	Volumetric stress tensor	MPa

$\boldsymbol{\epsilon}$	Strain tensor	$-$
ϵ_M	Mechanical Strain	$-$
ϵ_t	Thermal Strain	$-$
μ	Friction coefficient	$-$
$\boldsymbol{\sigma}$	Stress tensor	MPa
σ_0	Yield stress	MPa

1 Introduction

This study is about modeling of a clip connection. In this chapter the background of the problem, the limitations and the objective of the study is presented.

In this study is a clip joint studied. This is one way of connecting different parts together in a similar way as screw joints. The main idea is that a clip is fixed on a flat tower on one of the parts and then put into a hole on the other part to fix the parts together.

1.1 Background

The background for this Master Thesis is that a lot of companies is going towards a fully Simulation Driven Design with the intention of reducing the lead time and by that the costs of their products. For this to be possible the simulation models needs to correlate well to the reality but still simple to reduce costs of the simulations. Today is the behavior of clips not captured in a satisfying way in the simulations when having a simple model of the clip connection. The clip connection is of great interest since it is widely used in the automotive industry where many parts are connected by different types of clips.

A clip can be constructed by different materials but in the automotive industry it is common to use either plastic or metal, see Figure 1.2. The clips can be integrated in the parts or mounted on a small tower. The other end of the clip is mounted either in a rectangular hole, see Figure 1.3b, or around a cylinder on the other part.

Figure 1.1: *Example of parts connected with the studied clip.*

The problem today is that Volvo Car Corporation (Volvo Cars) do not have a good model to predict the behavior of the clip in FE-simulations. The clip studied in this report is used to connect e.g. the interior parts shown in Figure 1.1. When the interior is subjected to loads, e.g. temperature loads, it gets deformed and since it is connected with the clips the behavior of the interior is dependent on the clip behavior. This results in that to be able to predict the interiors behavior a good model of the clip connection is needed. The important properties to capture are the stiffnesses, friction and the force to assemble and release the clip joint.

(a) *An example of a plastic clip.*   (b) *The clip that is studied.*

Figure 1.2: *Different common clip types.*

1.1.1 Function of the clip

The metal clips are mounted or clamped by pre-tension on a tower. The clip stays because of the friction and that small thorns is digging in to the tower, see Figure 1.3a. After that the clip is mounted on the tower it is snapped in a hole in the other part. The hole is wider than the clip so it can move sideways with some friction. When mounted in the hole the clip is prevented from being released by being snapped under an edge in the part it is mounted in, see Figure 1.3b. This makes that it needs a force to disassemble the parts. One clip joint including both the tower and hole is shown in Figure 1.3c.
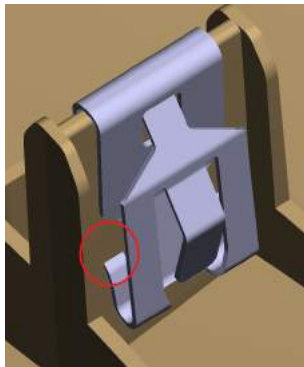
(a) *Illustration of how the clip is mounted on the tower.*   (b) *Illustration how the clip is snapped in the gap.*   (c) *Picture of a cut out of the assembled clip connection.*
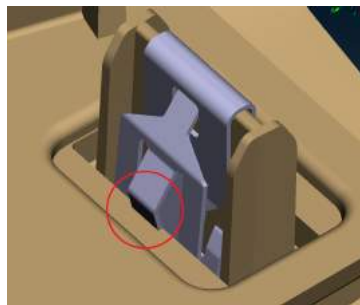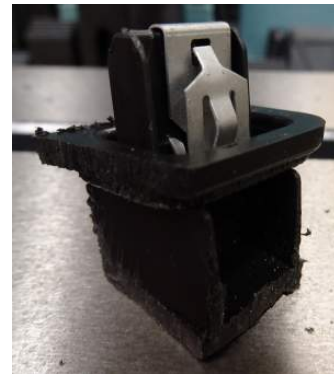
Figure 1.3: *Function of the clip.*

The clip that is studied in this report is of steel and the holes and towers is made in Acrylonitrile Butadiene Styrene (ABS) and Polypropylene (PP) plastic. Mostly the tower is of PP and the material around the hole is of ABS. A few physical tests are done with tower of ABS and material around the hole of PP to get a hint of the difference. In the different materials there is a variation of the width of the hole and also of the length of the hole so that the clip can move a different length in friction. The clips that are studied here are the non-guiding clips but in reality some clips are guiding clips and have not the same flexibility as the other clips, see Figure 1.4. These are used to guide the parts in a specific position as basic position. The guiding clips have not the same parameters and the same parameter values as the other clip and are not studied here.
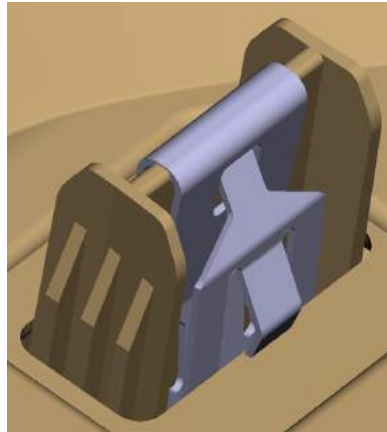
Figure 1.4: *Picture of a guiding clip.*

To simulate problems including clips using the Finite Element Method (FEM) it is common in the automotive industry to use Abaqus. This software includes a connector element that can be adopted with different behaviors and therefore will this program be used as a solver in this study. For setting up the models and to process the results is Ansa and Meta used, [1]. The procedure is shown in Figure 1.5.
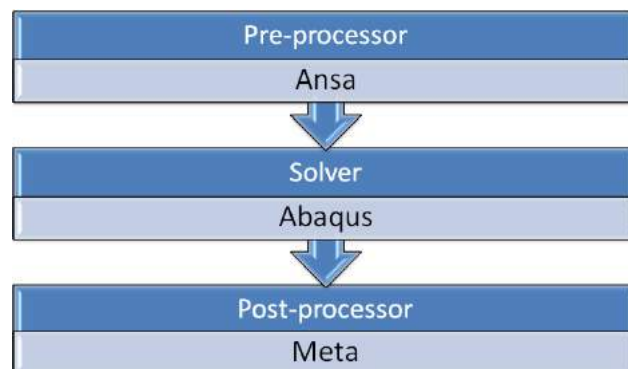
Figure 1.5: *Flowchart of the FEM programs used.*

1.1.2   Coordinate system

A coordinate system is defined in the clip connection. The x-direction is along the hole, the y-direction is along the width of the hole and the z-direction is out of the clip connection, from base of the tower to the top, Figure 1.6.
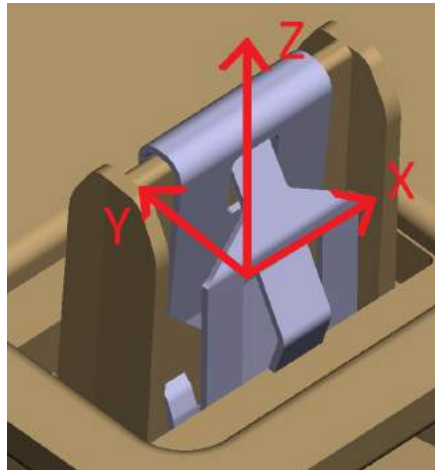
Figure 1.6: *The definition of the coordinate system of the clip joint.*

1.1.3 Evaluated parameters

The parameters to be tested are based on a discussion with experienced engineers and evaluated based on the design of the clip connection. The first parameter to evaluate is the force needed to assemble the clip. In simulations this value is not of interest but good to know in the actual assembly process of the parts. In the x-direction is where the largest movement is possible due to a gap and the parameter that is preventing this movement is the friction that will be evaluated.

The stiffness in the y-direction is evaluated together with rotational stiffness around the y and z-axis. The stiffness around the x-axis is not evaluated due to that it probably will be much higher than in the other directions based on the configuration. The last thing that is evaluated is the force that is required to dis-assemble the connection together with the stiffness in this direction. In addition to the parameters is the range of possible movement for the clip in the translation and rotational directions measured and implemented.

1.1.4 Previous Work

One common way of modeling the clip connection today is to model the connection only as rigid beam or spring element between the two nodes that correspond to the connection. The closest nodes to the connected node on each part is rigid connected to the connected node, see Figure 1.7, [2]. The rigid connection of the closest nodes to the connection node is called a Spider. If the connection is used in for example a crash simulation it can be added that the rigid connection between the parts is released at a specified value of the force in the connection element.

Previously Volvo Cars have done some small testing for the studied clip that is presented in Appendix A. Under this tests only friction along the hole and one rotation stiffness where tested and the other directions was assumed to have no motion. Under friction testing the clip dug in to the plastic around the hole due to the test setup.
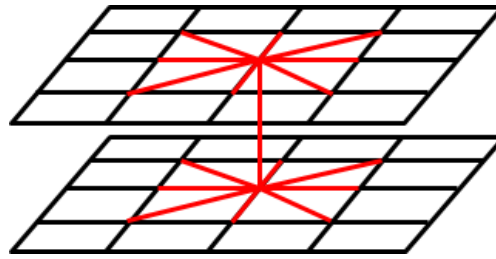
Figure 1.7: *The way of modeling clip joint with beam elements. The red lines represent beam elements and the black the element mesh.*

1.2 Purpose

The purpose is to investigate and find a simple model that can be used in finite element simulations to represent the clip connections. The model should be so simple that it can be used in the ordinary development work at companies but also represent the reality well. The main focus is on developing a model able to accurately capture the mechanical behavior of a selected metal clip under different temperatures, see Figure 1.2b. The model should primarily work in simulations with temperature loads. The model should be calibrated against performed measurement and detailed FEM-models, see Figure 1.8. A sensitivity analysis is also performed to investigate the variation of the parameters when varying parameters, e.g. the width of the hole, in the clip connection.
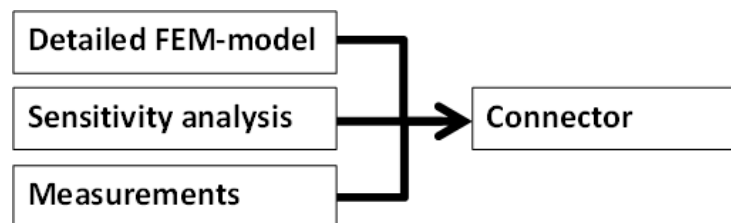
Figure 1.8: *The parts to reach a connector model to represent the clip joint.*

1.3 Limitations

In this report the clip shown in Figure 1.2b is studied. The objective is not to modify the clip but rather to find a good model for the existing one. The model will not be tested for implementation in a simulation with more than one clip. The experiment that are preformed is limited by the precision of the equipment that are available and the amount of test parts that are available. In this report manly clip connected into hole surrounded by ABS plastic is considered. A small study of the difference with PP is performed. The guiding clips are not studied. In the study is no coupling between the different parameters considered.

2 Theory

In this chapter the theory used to solve the problem is presented. The material properties are also presented in this chapter.

2.1 Basic mechanics

In this section the basic mechanics relevant to this study is presented. The presented areas are the mechanics of the properties in the clip connection and the basics of temperature loads, friction and isotropic hardening of materials.

It is common that different properties such as friction, stiffness etc. depends on other parameters and properties. The temperature and time is common variables that most properties are depending on. In many cases are the variation not large and the dependence of temperature can be disregarded from. In some applications and if a more accurate solution is needed are the dependence taken in to consideration, [3]. The interdependence between different properties are difficult to evaluate in many cases but can be possible. In this study is the way to evaluate the interdependence of the properties not examined and the properties are assumed to be unrelated to each other.

2.1.1 Mechanical properties of clip

All the different mechanical properties depends on the stiffnesses of the steel, the interaction between the steel and plastics and the geometry of the clip. When loading the clip connection the loading can be an applied force that gives a displacement, as explained in this section. It is also possible to instead apply a displacement that gives the corresponding force. The mechanics behind both cases are the same and it is only a matter of choice how to see it.

Translational stiffness

The translational stiffness in the clip joint comes from when the hole around the clip is moved due to an applied load, F_a, and the tower is stacked in its position, see Figure 2.1. In this case is the clip compressed and the relation between the applied force and the displacement gives the stiffness at that force, see equation (2.1), [4]. The stiffness can be constant for all different applied forces or be dependent on the applied force so that the force-displacement relation is nonlinear.

$$dy = \frac{F_a}{k_t} \tag{2.1}$$

where F_a is the applied force, k_t is the stiffness and dy is the resulting displacement.
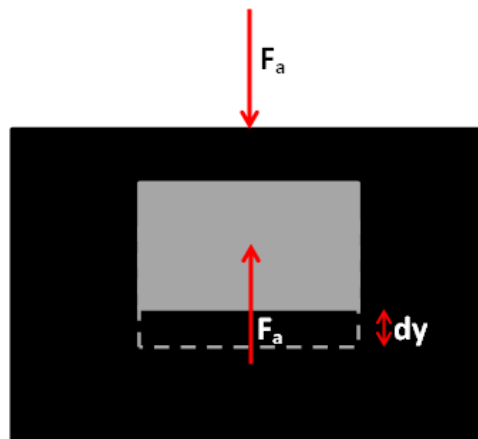
Figure 2.1: *Illustration of equilibrium of a clip joint loaded in y-direction.*

Rotational stiffness

The rotational stiffnesses are based on that a torque is applied on the hole around an axis that passes through the center of the clip. This torque give raise to a rotation of the hole relative the tower. The relation between the applied torque and the displacement gives the rotational stiffness, see equation (2.2), [4]. One way of applying this torque is shown in Figure 2.2. In Figure 2.2 is a force, F_a, applied at a distance dx from the center and the same force is applied in the opposite direction in the center. The application of these forces gives a torque in the center on the hole that gives a rotation of the hole relative the tower.

$$d\theta = \frac{M_a}{k_\phi} = \frac{F_a dx}{k_\phi} \tag{2.2}$$

where M_a is the applied torque, k_ϕ is the rotational stiffness, dx is the distance to the center and $d\theta$ is the resulting rotation.
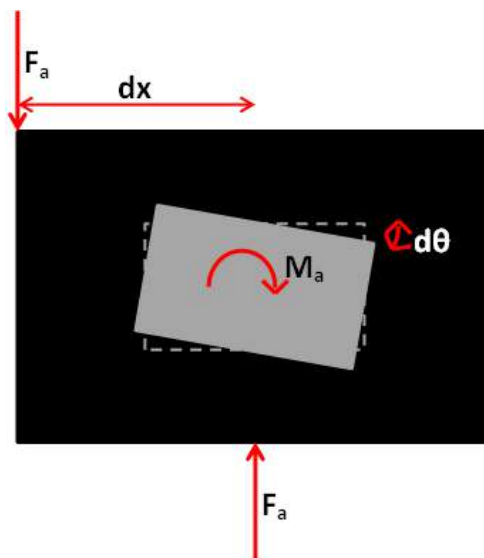
Figure 2.2: *Illustration of equilibrium of a clip joint loaded with a torque.*

Assembly and dis-assembly force

In the assembly process when the clip mounted on the tower is going in to the hole are the flanges compressed to fit into the hole, see Figure 2.3. The compression of the flanges creates a stiffness in the assembly. When the flanges are compressed enough to fit in the hole is the force for the continuing assembly decreasing because the force to overcome now is the friction between the hole and the clips flanges. The clip is forced to continue assembly to the static equilibrium position when the flanges has passed over the corner of the hole. This happens due to the release of the energy saved in the flanges from the compression. The assembly force, F_{ass}, is defined as the maximum value of the force that occur when the flanges enter the hole and friction takes over. The dis-assembly process is similar to the assembly process, first compression of the flanges, then friction and last realize of the clip.
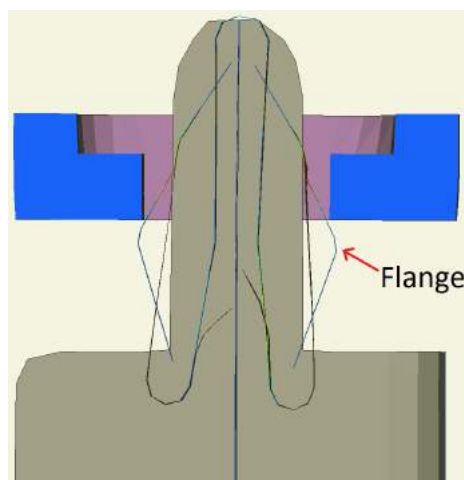
Figure 2.3: *Figure of the assembly and dis-assembly of the clip connection.*

2.1.2 Tribology

When two bodies are in contact this gives raise to a normal force, F_N, between the bodies. The normal force is in the normal direction between the surfaces that are in contact. In Figure 2.4 is one example of a free body diagram between two bodies in contact with an applied load, F_a, on one of the bodies. The other body is fixed. In Figure 2.4 represents F_t the tangential force that occur due to the friction between the bodies.
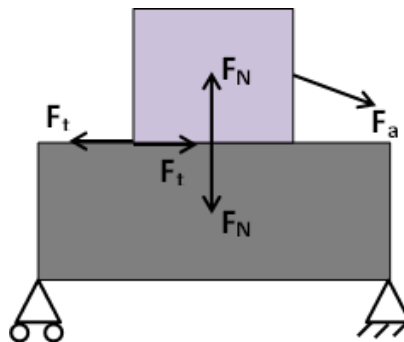
Figure 2.4: *An example of the normal- and friction forces between two bodies.*

The tangential force can as maximum reach the friction force that is $|F_f| = -\mu F_N$, [4]. The friction force depends on the friction coefficient, μ, that is depending on the surface roughness of the materials that are in contact. The surfaces that are in contact are slipping against each other if the tangent force, F_t, is equal to the friction force, F_f. If the tangent force is smaller than the friction force the surfaces are stacked to each other. When they are stacked to each other can some stiffness, as explained in Section 2.1.1, in the tangential direction exist. For more information about the friction model see [5]. The friction coefficient between the materials that is used are presented in Table 2.1. These general values are valid between the materials but the friction coefficient varies depending on how the parts are produced and on the temperature. Hence these values are approximate for this application.

Table 2.1: The friction coefficients between different materials. [6]

Materials	μ
PP-Steel	0.36
ABS-Steel	0.3
Steel-Steel	0.31

In the studied clip joint exist a pre-tension in the clip when assembled that gives rise to a normal force and thereby a friction force that needs to be exceeded for sliding. This normal force can in practice be changed if the clip joint is loaded in y direction or by a torque around z-axis, but this is disregarded from.

2.1.3 Temperature load

An increase or decrease in temperature from the stress free state is a type of loading for the structure due to that the material is expanding or contracting. This creates stresses in the material if the material cant expand in the way that it wants to. The distance that the material wants to expand is dependent on more than the temperature change. The thermal strain is also dependent on the materials thermal expansion coefficient, α. The relation between the strain in the material and the temperature is shown in equation (2.3), [3]. The temperature change give only normal strains and not any shear strain. The total strain is the sum of the thermal and the mechanical strain, see equation (2.5). The mechanical strain is the strain that the stress in the material is dependent on from the kinematics, see equation (2.4), [7].

$$\epsilon_t = \alpha \Delta T \tag{2.3}$$

$$\epsilon_M = \frac{\sigma}{E} \tag{2.4}$$

$$\boldsymbol{\epsilon} = \boldsymbol{\epsilon_M} + \boldsymbol{\epsilon_t} \tag{2.5}$$

α is the thermal expansion coefficient, ΔT the temperature difference, ϵ_t the thermal strain, σ is the normal stress, E is the young's modulus, ϵ_M is the mechanical strain and ϵ is the total strain.

2.1.4 Isotropic hardening

Isotropic hardening together with kinematic hardening is the most common models to model the plasticity of materials. Isotropic hardening is based on that the yield stress is increasing or decreasing when the plastic strain is increasing. The isotropic hardening model is explained in this section.

The strain in the material can be divided into one elastic and one plastic part, see equation (2.6), [8]. The stress can instead be divided into one volumetric and deviatoric part, see equation (2.7).

$$\boldsymbol{\epsilon} = \boldsymbol{\epsilon_e} + \boldsymbol{\epsilon_p} \tag{2.6}$$

$$\boldsymbol{\sigma} = \boldsymbol{\sigma_{dev}} + \boldsymbol{\sigma_{vol}} \tag{2.7}$$

where $\boldsymbol{\epsilon_e}$ is the elastic strain tensor, $\boldsymbol{\epsilon_p}$ is the plastic strain tensor, $\boldsymbol{\sigma_{dev}}$ is the deviatoric stress tensor and $\boldsymbol{\sigma_{vol}}$ is the volumetric stress tensor.

The relation between the stress and strain in the material is shown in equation (2.8).

$$\boldsymbol{\sigma} = \boldsymbol{E}(\boldsymbol{\epsilon} - \boldsymbol{\epsilon_p}) \tag{2.8}$$

where is $\boldsymbol{E}$ is Young's modulus.

The elastic strain in the new time step is calculated as in equation (2.9).

$$\hat{\boldsymbol{\epsilon}} = \boldsymbol{\epsilon_{old}} + \boldsymbol{\Delta\epsilon} \tag{2.9}$$

where $\boldsymbol{\Delta\epsilon}$ is the elastic strain increment tensor and $\boldsymbol{\epsilon_{old}}$ is the strain tensor from previous time step.

The yield condition for the rate independent material is as in equation (2.10).

$$\sqrt{\frac{3}{2}\boldsymbol{\sigma_{dev}} : \boldsymbol{\sigma_{dev}}} = \sigma_0 \tag{2.10}$$

where σ_0 is the yield stress and can be dependent on the temperature and the plastic strain.

The scalar plastic strain increment is solved from equation (2.11) and equation (2.12). For rate independent material is the solution linear to solve but for rate dependent materials need it to be solved with Newton's method, [9].

$$\tilde{\epsilon} - \Delta\epsilon_{pl} - \frac{\sigma_0}{3G} = 0 \tag{2.11}$$

$$\tilde{\epsilon} = \sqrt{\frac{2}{3}\hat{\epsilon} : \hat{\epsilon}} \tag{2.12}$$

where G is the shear modulus.

The deviatoric stress in current time step is calculated according to equation (2.13).

$$\boldsymbol{\sigma_{dev}} = \frac{2G}{1 + \frac{3G}{\sigma_0}\Delta\epsilon_{pl}}\hat{\epsilon} \tag{2.13}$$

The plastic strain increment is shown in equation (2.14) and can be solved with the deviatoric stress from equation (2.13).

$$\boldsymbol{\Delta\epsilon_{pl}} = \Delta\epsilon_{pl}\frac{3\boldsymbol{\sigma_{dev}}}{2\sigma_0} \tag{2.14}$$

2.2 Material properties

The materials of interest in this report are steel and the plastics ABS and PP. Material properties are presented below.

2.2.1 Steel

Steel is a material with high density and a low expansion coefficient. The steel that is used in the clip has a thermal expansion coefficient of $1.2 \cdot 10^{-5}$ $1/^{\circ}C$, Poisson's ratio of 0.3 and the Young's modulus is 210 GPa at room temperature, [10]. The properties are assumed to be constant over the temperature.

2.2.2 Acrylonitrile butadiene styrene

The plastic ABS have a higher thermal expansion coefficient than steel which also are typical for all plastics. The expansion coefficient for ABS is $6.5 \cdot 10^{-5}/^{\circ}C$. Young's modulus for the used ABS are 2.2 GPa, provided by Volvo Cars. The plasticity for this plastic can be approximated to be isotropic. The Poisson's ratio is assumed to be constant 0.4 at all temperatures since the temperature dependence is very small.

2.2.3 Polypropylene

PP has roughly the same properties as the ABS but yields at a lower stress. The isotropic plasticity behavior is also valid for PP. The Young's modulus for PP is approximately $2, 3$ GPa and Poisson's ratio 0.4 for all temperatures, provided by Volvo Cars.

2.3 Basics of Finite Element Method

The FEM is a way to numerically solve differential equations by discretizing the domain into a mesh of elements and in engineering it is specially used to solve the equations of solid mechanics to get the displacement and stresses that a given load on one or more connected bodies creates, [7]. The FEM equations are established by assembling the contributions from local elements generated by a mesh. The elements can have only one node but it is often more and can in theory be any number. An element with a given number of nodes can also have different number of Degrees of Freedom (dof) depending on the polynomial order that are approximating the displacement filed in the element. The number of dof are also depending on the number of independent dof in each node, the independent translational and rotational direction. For an element with two nodes that has dof in all three rotational and three translational directions gives six dof in each node and they are connected by the properties of the elements. One of the simplest elements is a rigid beam element that prescribes the two nodes to have the same displacement and rotations.

2.3.1 Dynamic analysis

One of the equations that can be solved with FEM is the equation of motion, see equation (2.15).

$$M\frac{\partial^2 \boldsymbol{u}}{\partial t^2} + C\frac{\partial \boldsymbol{u}}{\partial t} + \boldsymbol{K}\boldsymbol{u} = \boldsymbol{f} \tag{2.15}$$

where $\boldsymbol{M}$ is the mass matrix, $\boldsymbol{C}$ is the damping matrix, $\boldsymbol{K}$ is the stiffness matrix, $\boldsymbol{f}$ is the external force and torque vector and $\boldsymbol{u}$ is a vector containing the displacements and rotations.

The equation of motion, equation (2.15), can be rewritten in terms of the internal, $\boldsymbol{I}$, and external forces, $\boldsymbol{f}$, see equation (2.16).

$$M\frac{\partial^2 \boldsymbol{u}}{\partial t^2} = \boldsymbol{f} - \boldsymbol{I} \tag{2.16}$$

where

$$\boldsymbol{I} = C\frac{\partial \boldsymbol{u}}{\partial t} + \boldsymbol{K}\boldsymbol{u} \tag{2.17}$$

In this case is the problem dependent on time and needs to be solved with an explicit or implicit method. The difference between the implicit and explicit methods is that the explicit method only use information from the known previous time step and solves the next time step from that to update the configurations, velocity and accelerations, [11]. The implicit methods are doing the same but adds on that the sought for configuration not only depend on the previous time step but also unknown entities at the current time step and this nonlinear equations is solved using for example Newton's iterations. In this study is the explicit method used.

Explicit solution procedure

The basic of the explicit solution procedure is Taylor series expansion, [11]. There exist different versions on the explicit solution procedure but here is only the one adoptive explained. For the presented procedure to be computational effective a lumped mass matrix is needed for a simple inversion. This can be achieved in some different ways but one common way is to sum up the rows in the original mass matrix, [12]. The presented solution procedure uses the mid-increment, $(i \pm \frac{1}{2})$, values that is the values between two time steps. To begin with is mid-increment of the velocity between the next and previous time step computed as shown in equation (2.18), [9].

$$\frac{\partial \boldsymbol{u}}{\partial t}^{(i+\frac{1}{2})} = \frac{\partial \boldsymbol{u}}{\partial t}^{(i-\frac{1}{2})} + \frac{\Delta t^{(i+1)} + \Delta t^{(i)}}{2} \frac{\partial^2 \boldsymbol{u}}{\partial t^2}^{(i)} \qquad (2.18)$$

where $\Delta t^{(i)}$ is the time step i.

From this the displacement at the next time step is computed, see equation (2.19).

$$\boldsymbol{u}^{(i+1)} = \boldsymbol{u}^{(i)} + \Delta t^{(i+1)} \frac{\partial \boldsymbol{u}}{\partial t}^{(i+\frac{1}{2})} \qquad (2.19)$$

With this can the internal force be computed as shown in equation (2.16) and the acceleration in the next time step, see equation (2.20).

$$\frac{\partial^2 \boldsymbol{u}}{\partial t^2}^{(i+1)} = \boldsymbol{M}^{-1}(\boldsymbol{f}^{(i+1)} - \boldsymbol{I}^{(i+1)}) \qquad (2.20)$$

For the first mid-increment value of the velocity is instead equation (2.21) used because the velocity before time zero is not known.

$$\frac{\partial \boldsymbol{u}}{\partial t}^{(\frac{1}{2})} = \frac{\partial \boldsymbol{u}}{\partial t}^{(0)} + \frac{\Delta t^{(1)}}{2} \frac{\partial^2 \boldsymbol{u}}{\partial t^2}^{(0)} \qquad (2.21)$$

Time step

For the explicit method to be stable a sufficiently small time step is needed, but if a too small time step is used the solution process takes very long time and gets expensive. The usual way of determine a appropriate time step is to make sure that the information cannot pass one element under the time step. The time step too use is determined from the smallest time step from equation (2.22) of all elements, [13].

$$\Delta t = \frac{L_e}{c} \qquad (2.22)$$

were L_e is the characteristic element length and c is the wave speed in the material.

2.3.2   Constraint modeling

A constraint between two parts that occurs during simulation can be modelled using the Penalty method. This method is based on that a large stiffness, ξ, is added for each dof that is in contact, [14]. The function that determines the additional constraint can be collected in a matrix, $\boldsymbol{h}$, and is sought to be zero. The constraint that needs to be fulfilled can for example be bodies in contact or friction sticking between parts. The additional constraint can be divided with the constraint matrix $\boldsymbol{P}$ and the matrix $\boldsymbol{q}$ containing the prescribed displacements, see equation (2.23), [15].

$$\boldsymbol{h} = \boldsymbol{P}\boldsymbol{u} - \boldsymbol{q} \tag{2.23}$$

After adding this constraint in to the dynamic equation of motion the equation is changed to equation (2.24).

$$\boldsymbol{M}\frac{\partial^2 \boldsymbol{u}}{\partial t^2} + \boldsymbol{C}\frac{\partial \boldsymbol{u}}{\partial t} + (\boldsymbol{K} + \xi \boldsymbol{P}^T \boldsymbol{P})\boldsymbol{u} = \boldsymbol{f} + \xi \boldsymbol{P}^T \boldsymbol{q} \tag{2.24}$$

2.3.3   Temperature Change

If the temperature is changing from the stress free state adds this a loading as explained in Section 2.1.3. In the finite element formulation, see equation (2.15), adds this an external loading term to $\boldsymbol{f}$ that is dependent on the temperature change. The added term is shown in equation (2.25).

$$\int_{\Omega} \boldsymbol{\sigma}(\boldsymbol{\epsilon_t}) : \boldsymbol{\epsilon}(\delta\boldsymbol{u}) \ d\Omega \tag{2.25}$$

where $\delta\boldsymbol{u}$ is the test functions, $\boldsymbol{\sigma}(\boldsymbol{\epsilon_t})$ is the stress from the temperature strain and Ω is the domain of the problem.

2.4   Connector element

In Abaqus exist some different elements that can be used to connect different parts to each other but they are suited for different applications. For example there is a spring element that works well for springs but can only be used for that. One element that connects two points with many different properties is the connector element, [16]. This element has different parameters that can be controlled and is thereby chosen to represent the clip joint. The mechanical behavior that are controlled in the connector element are distributed as in Figure 2.5.
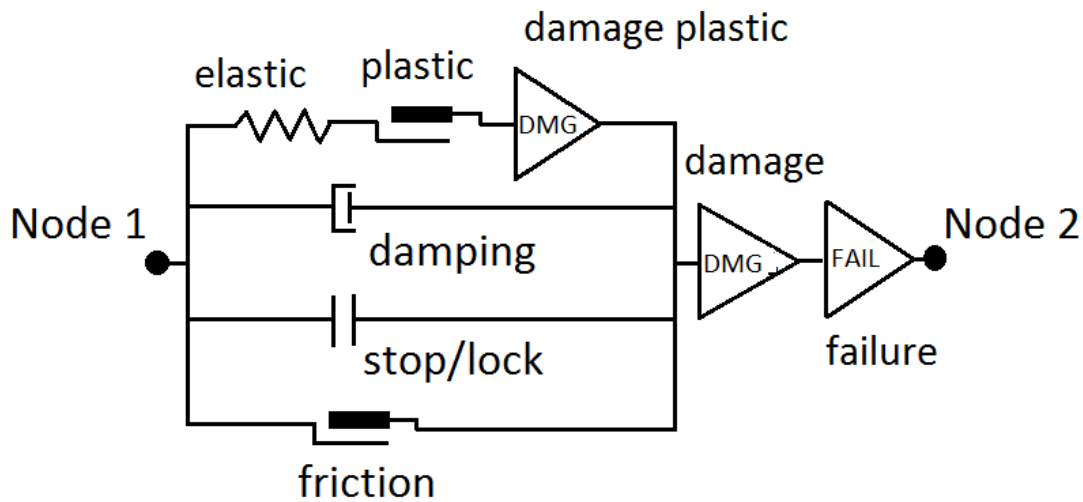
Figure 2.5: *The conceptual illustration of connector behavior. Redrawn from [16].*

This distribution exists in all three translational directions and also in the three rotational direction. The coordinate system that this is valid for can be chosen in any direction and does not need to be located so that one axis is located along the line between the two nodes. It can be a fixed coordinate system that is constant in its direction during loading or a coordinate system that follows a deformation or a node. Since the mechanisms are distributed in a specific way it may be necessary to combine two connector elements to get the behavior of the connection that is sought for. This is illustrated in Figure 2.6 for combining two elements in parallel and in Figure 2.7 for two elements in series.
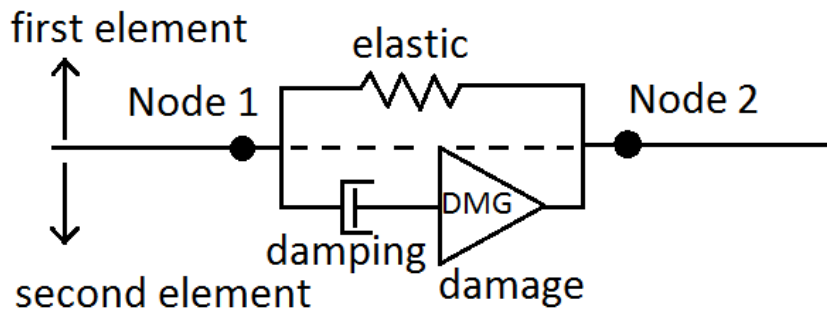

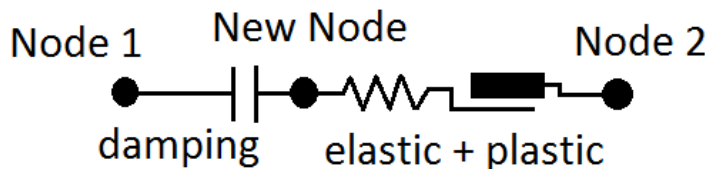Figure 2.6: *The conceptual illustration of parallel connector elements. Redrawn from [16].*

Figure 2.7: *The conceptual illustration of connector elements in sequence. Redrawn from [16].*

2.4.1 Connector parameters

One of the parameters in the connector element that can be calibrated is the elasticity that represents the same behavior as a spring in translational direction and a torsional spring in the rotational direction. It is also possible to calibrate a damping of the element and a plastic behavior. The plastic behavior can be for example hardening or softening. The connection makes it possible to add a friction and to set up a lock or stop in the connection. The lock and stop can lock a component from moving at a specific deformation of the connection or to stop the connection from moving at all in one direction. The damage can not only be defined for the elasticity but also for the whole connection and depend on many different variables, e.g. the displacement or applied force. The last parameter that can be defined in the connection is failure. The failure can be on a specific component or the whole connection, [16].

The different parameters can be calibrated so that it can depend on other parameters both in the connection and field variables, e.g. temperature, in the whole problem. For example can the friction of the connection be dependent on the temperature as is illustrated in Figure 2.8a. It is also possible to have a stiffness that is linear until a specific value of the local force and then go to zero. This is illustrated in Figure 2.8b.
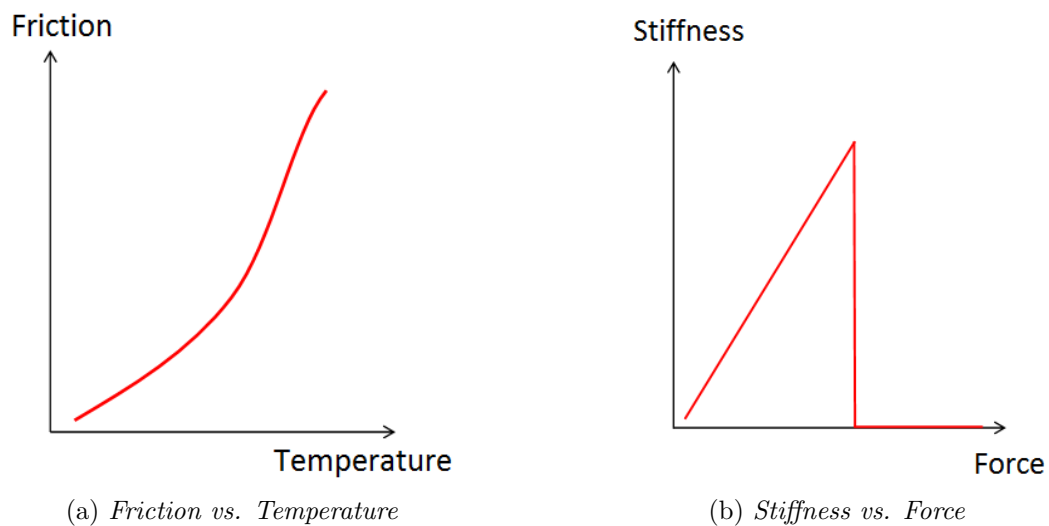

(a) *Friction vs. Temperature*   (b) *Stiffness vs. Force*

Figure 2.8: *Example of possible parameter dependence.*

3 Method

In this chapter the method that was used to investigate the properties of the clip joint presented. The test was prepared and performed in parallel to component simulations. The results from the simulations and the tests are compared and from this are the values of the parameters decided. The decided parameters are implemented in a simple element that can represent the clip joint.

3.1 Physical testing

In this section is the test setups and the method of performing the tests presented. In the testing we tried to minimize the effects of the deformation of the hole and tower but still have the friction and the motion of the clip as realistic as possible.

3.1.1 Measurement setup

The testing was first done in room temperature to capture the behavior at this temperature. After that was the same testing done at approximately $80°C$. The heating was accomplished in a climate chamber to $90°C$ and then the test was performed outside in room temperature. The time from taken the test pieces out of the climate chamber until the test was finished was approximately 1-2 minutes. The assembly is always done at room temperature in practice. Because of this is the assembled clip connection heated and the assembly force at $80°C$ not measured.

The performed test was displacement controlled. The displacement was manually controlled from a coordinate table with a precision of 0.01 mm and then transferred by a force sensor to the selected place of the test piece, see equipment in Figure 3.1. The other end of the test piece was fastened in a vise. The force needed to impose the displacement was read by the force sensor and tracked from the program Dasylab in the computer, [17]. The force vs. displacement was manually picked from a movie that tracked both the applied displacement and force at the tests.

Figure 3.1: *The test equipment that was used.*

The test material was processed by cutting out the tower so that only the two edges around the tower was included, see Figure 3.2a. The hole is surrounded by a stiffening just around the hole, see Figure 3.2b. For the component test the hole was cut out at the end of the thicker part. The parts that were sawed out creates together the test piece, see Figure 3.2c. In total 12 test pieces were used for the stiffnesses and friction measurements and five for the assembly and dis-assembly force measurements. All the tests performed used this test pieces. To understand the possible variations the width of the holes were measured at the tests.
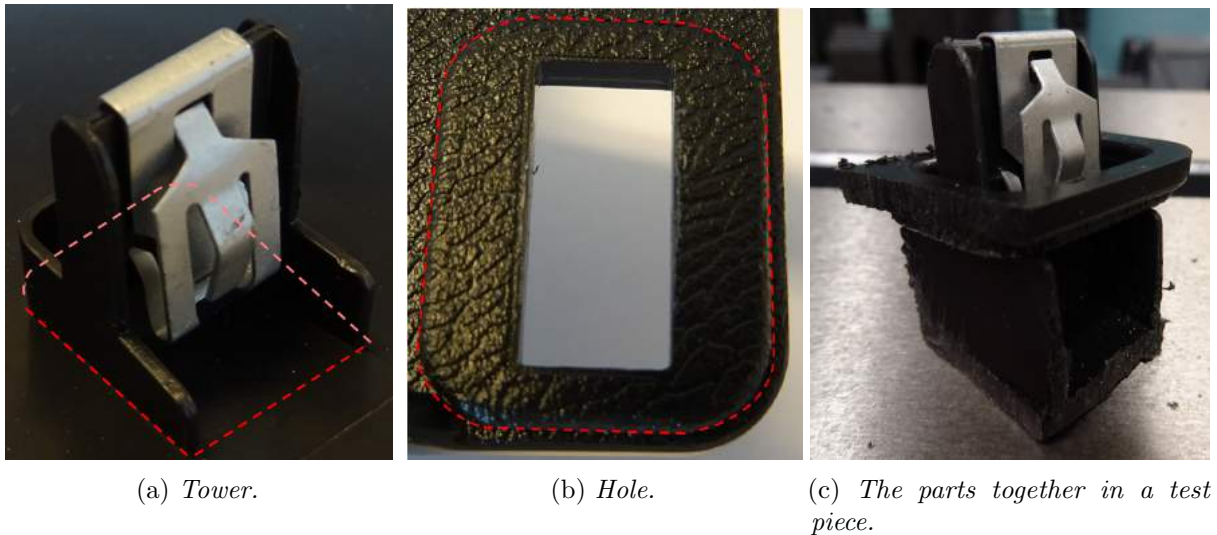

(a) *Tower.* (b) *Hole.* (c) *The parts together in a test piece.*

Figure 3.2: *The processed parts for material testing.*

3.1.2 Assembly and dis-assembly

To measure the assembly force, F_{ass}, the hole was fastened in the vise but first it was reinforced on the cutting edges with chemical metal in order to prevent the hole from deforming when it is fastened. After fastening the hole the top of the tower was placed in the hole and the tip on the force sensor was put in the base of the tower, see Figure 3.3. To make sure the force stays in the center of the base a small hole was drilled to guide the tip of the sensor to stay in that position under the loading. The loading was done by moving the force sensor to push the clip in to the hole while the force was measured.

Figure 3.3: *The test configuration of the assembly measurement.*

The force for dis-assembly, F_{dis}, was measured similar to the assembly with the reinforced hole fastened in the vise. Instead of loading in the bottom of the tower the displacement was applied with the force sensor at the top of the clip so it comes at the right direction, see Figure 3.4. Since the top is very narrow it was not possible to have a tip applying the force to the clip. Instead the flat area at the force sensor was used so that it does not matter if the tip is moving half a millimeter under the loading, the displacement is still applied in the right way, see theory in Section 2.1.1.

Figure 3.4: *The test configuration on the dis-assembly measurement.*

3.1.3 Friction and translational stiffness

The setup for measuring the force, F_f, that is needed to overcome the friction, see theory in Section 2.1.2, was done by fixing the base of the tower in the vise and then apply a displacement via the force sensor. The tip applies the load at a point that lies in the center of the hole side, see Figure 3.5a. This ensures that the hole is translating and not rotating.

(a) *The test configuration for friction test.*   (b) *The test configuration for measurement of stiffness in y-direction.*

Figure 3.5: *Translational test configurations.*

The translational stiffness, k_t, in the y-direction was measured in the same way as the friction and the only difference is that the tower is rotated 90 degree in the vise, see theory in Section 2.1.1. The force was applied on the long edge that corresponds to the right loading direction, see Figure 3.5b.

3.1.4   Rotational stiffnesses

The rotational stiffness, k_ϕ, around the z-axis was measured in the same way as the translational stiffness but the displacement was not applied in the center of the edge but instead at a measured distance from the center, see Figure 3.6b. The loading gets not only rotational but also some influence from the stiffness in y-direction. This was due to that it was not possible with available resources to have a counter force that prevent translation at the center of the opposite side. The force that is measured can be transferred to a torque, see Section 2.1.1.

To measure the last parameter, the rotational stiffness around the y-axis, the same setup was used. The only difference is that the test pieces is rotated $90°C$ and the displacement was applied at the top of the hole at a distance from the center, see Figure 3.6a.

(a) *The test configuration for measuring the rotational stiffness around the y-axis.*
(b) *The test configuration for measuring the rotational stiffness around the z-axis.*

Figure 3.6: *Rotational test configurations.*

3.1.5   Test to see influence of the plastic parts

To see what influence that the plastic parts have in friction is some additional tests performed. In this tests is a piece of metal glued to the edge of the hole, see Figure 3.7. At this plate is the force applied. This will prevent the edge from buckling and the tip of the force sensor from dug in to the plastic. This change is not used in all tests due to that it can change the behavior and might include new uncertainties.
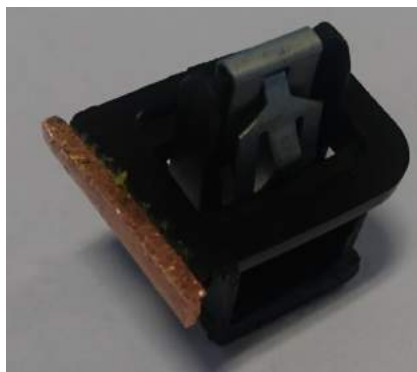

Figure 3.7: *Test piece with metal plate on the edge.*

3.1.6 Tests with different materials

To get an overview of how much the parameters is depending on the material of the tower and hole a few tests was done with the hole surrounded by PP and the tower in ABS. This is done in the same way as the other tests and the only difference is the materials and that the length of the hole is greater for this material combination. The most important parameter to look for is the difference in the friction.

3.2 Numerical simulations

In this section are the setup and method for the simulations and how the connector element that represent the clip joint is constructed described.

3.2.1 Detailed FEM-model

The detailed FEM-model, see Figure 3.8, was based on the geometry of the tower, clip and hole and the different materials and their properties, see Section 2.2. The detailed model was constructed with shell elements for the tower and the clip and with solid elements around the hole. Contact with friction coefficients, presented in Section 2.1.2, between the parts sliding on each other was added in the model. No friction between the tower and the hole were assumed due to that tower and hole in reality rarely are in contact. The loading was in all cases applied as a displacement or a rotation. The solver used is Abaqus explicit, see Section 2.3.1.

The detailed model was loaded by a controlled displacement on the tower to get the clip fastened on the tower, see Figure 3.8a. Under this loading the clip was held fixed. When the clip was assembled on the tower was the boundary conditions on the clip released. Instead the hole was hold fixed under the following loading on the tower, see Figure 3.8b. The force needed on the tower in the assembly process is measured.

When the FEM-model was assembled, see Figure 3.9, it was loaded in the x-direction to measure at what force the clip starts to slide. The assembled model was also loaded with a small displacement of the tower in y-direction. Rotational displacements around y and z-axis to measure the corresponding rotational stiffnesses were also applied. All the loadings were done from the assembled state. The last loading that was performed was in negative z-direction to measure the force needed to dis-assemble the clip joint. To get the same behavior as in reality the thorns shown in Figure 1.3a was stacked too the tower. The loadings were done at room temperature and all the results are filtered to reduce the noise in the explicit solution.
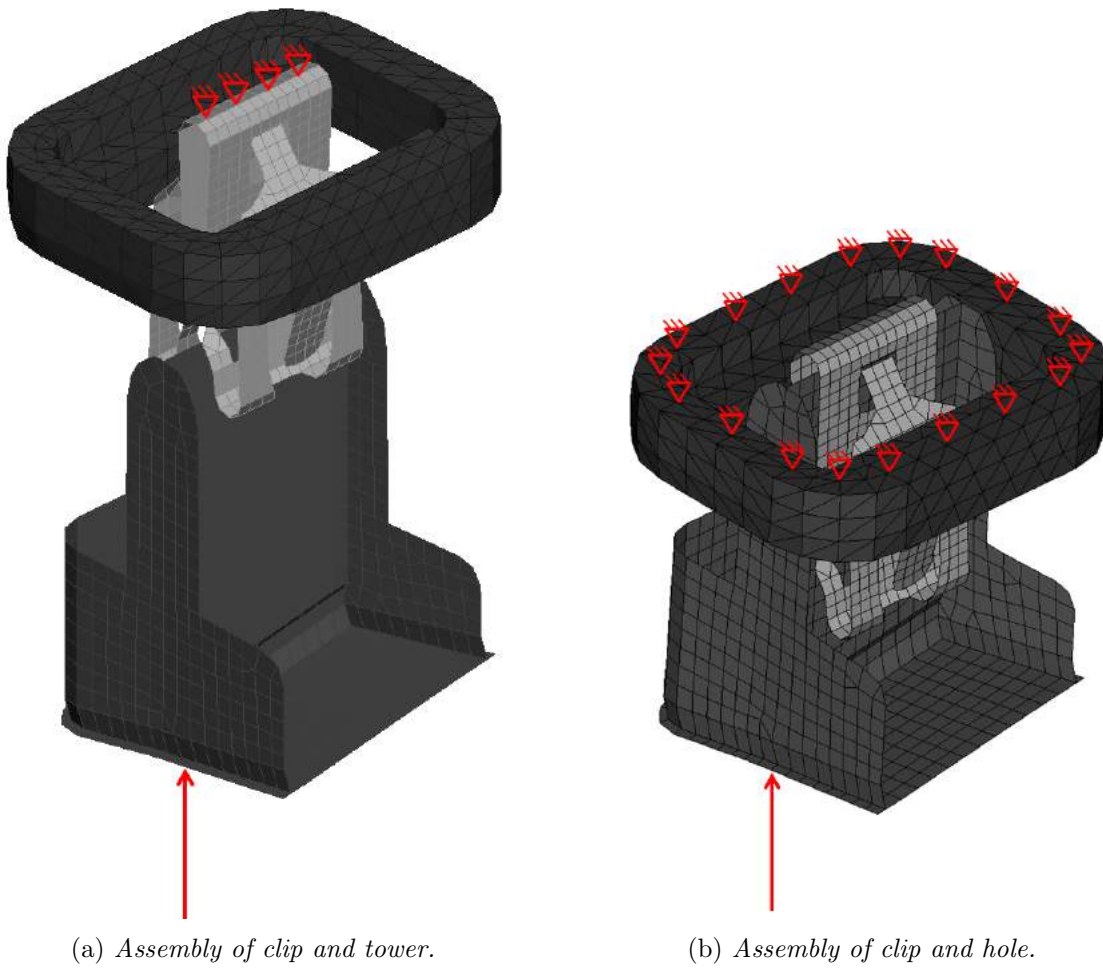
(a) *Assembly of clip and tower.*   (b) *Assembly of clip and hole.*

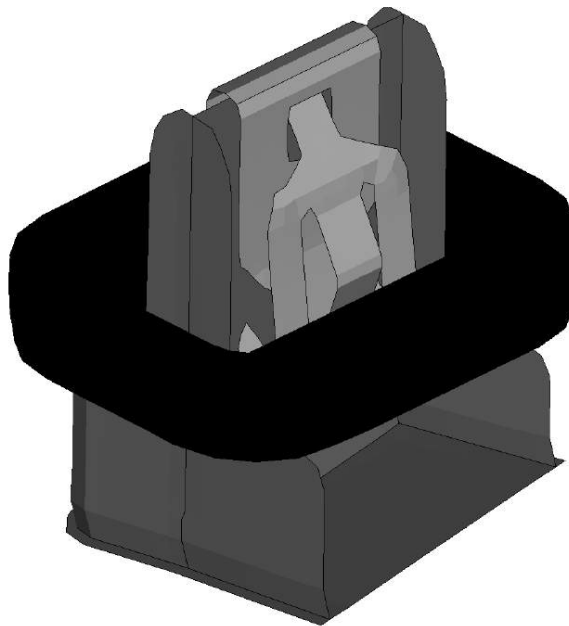Figure 3.8: *The boundary conditions under the assembly simulation.*

Figure 3.9: *The assembled detailed clip model.*

3.2.2   Sensitivity analysis

To capture how sensitive the FEM-model and thereby also the clip connection a sensitivity analysis was performed. The parameters that were varied is presented in Table 3.1 together with their nominal values and the changes of the FEM-model performed. In addition to this was also a longer loading time included in the sensitivity analysis.

Table 3.1: Parameter values to vary under sensitivity analyze.

Parameter	Nominal value	Change 1	Change 2
Target of mesh size of the clip	0.75 mm		0.5 mm
Element type on the clip	Reduced quad element	Quad element	
Thickness of clip	0.4 mm	0.45 mm (+12.5%)	0.35 mm (-12.5%)
Size of hole	8.5 mm	9 mm (+5.9%) 9.5 mm (+11.8%)	8 mm (-5.9%)
Friction coefficient between clip and hole	0.3	0.36 (+20%)	0.24 (-20%)
Friction coefficient between clip and tower	0.36	0.42 (+16.7%)	0.3 (-16.7%)
E-module of the clip	210 GPa	231 GPa	189 GPa
The clip assembly position	Center of tower	Clip moved 1mm	Clip and tower moved 1 mm each
Temperature change	23 °C	80 °C	

To capture how sensitive the model was for the different parameters they were varied one at a time and the change in the result was evaluated. It can be remarked that the friction coefficients that were changed in the sensitivity analysis represents the change from ABS plastic around the hole to PP and PP to ABS in the tower. It should also be noted that with the change of temperature was only the expansion of the materials considered, see Section 2.1.3, and the change in friction was not considered due to lack of data in its temperature dependence.

3.2.3   Connector model setup

The model was setup using the pre-post software Ansa, [1], and the deck for Abaqus that exist inside Ansa. A connector element was constructed between two defined nodes and in this element the behavior that was needed to match the decided behavior added. The two defined nodes are in an analysis connected to the nodes around the hole and tower with a spider, see Section 1.1.4, also called coupling constraint in Abaqus, [18]. The connection-type of the connector element was set to Cartesian and Cardan because this gives the possibility for the element to move in all direction and rotate around all axis without any constraints.

The behavior in the connector element was implemented with elasticity to represent the stiffnesses in all directions. The stiffnesses were implemented to depend on the temperature. The maximum movements are controlled by implemented stops that prevent further displacement after specific values. The friction behavior with sliding at a specific force was implemented with elasticity as a force vs displacement curve. The failure in the dis-assembly process was implemented with failure at a specific displacement.

The dependence of a parameter are defined in Abaqus as points in the graph. In Abaqus is this discrete points in the graph linearly interpolated. After the endpoint of the defined points is Abaqus continuing the dependence either by a linear extrapolation or a constant value from the other points, see Figure 3.10. The extrapolation of the parameters is set as linear extrapolation to get the most realistic behavior.
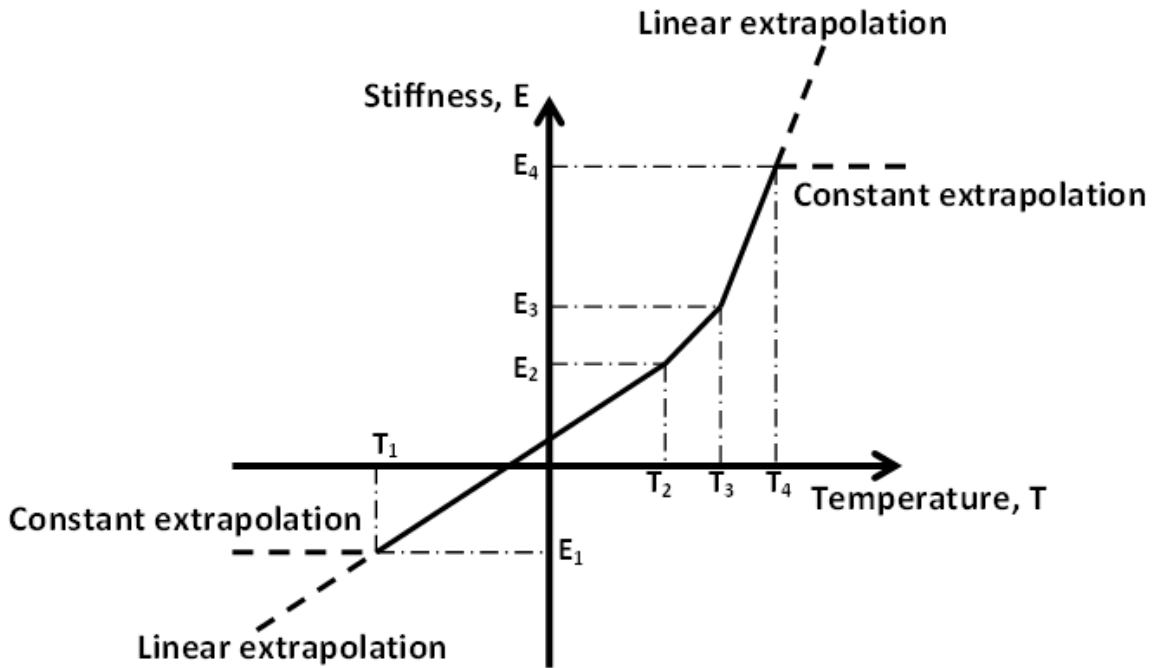

Figure 3.10: *The different types of extrapolation.*

4 Results

In this chapter the result from the tests and simulation are presented. The chosen values of the parameters in the simplified model are also presented.

4.1 Physical testing

In this section some selected representative tests are presented for the different parameters. In the figures both the tests at room temperature and $80°C$ are presented.

The measured assembly force, F_{ass}, versus the applied displacement for the performed tests is shown in Figure 4.1. Each curve represents one test and the doted black line represents the detailed simulation that are presented in Section 4.2. The dis-assembly force, F_{dis}, that are measured is shown in Figure 4.2. In this figure the blue curves represents the tests in room temperature and the yellow curves at $80°C$. The dependence between the required force and the applied displacement in the y-direction is shown in Figure 4.3.

The friction tests are presented in Figure 4.4 with the relation between the corresponding force and the applied displacement. The measured rotational stiffness around the y-axis, $k_{\phi y}$, is the gradient in the torque vs angels graph shown in Figure 4.5. The gradients in Figure 4.6 represents the measured rotational stiffnesses, $k_{\phi z}$, around the z-axis.
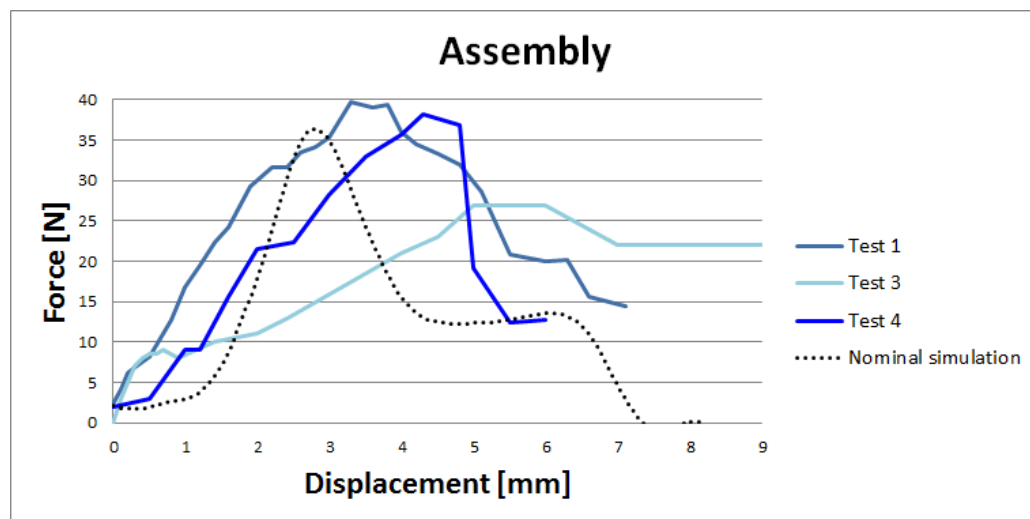

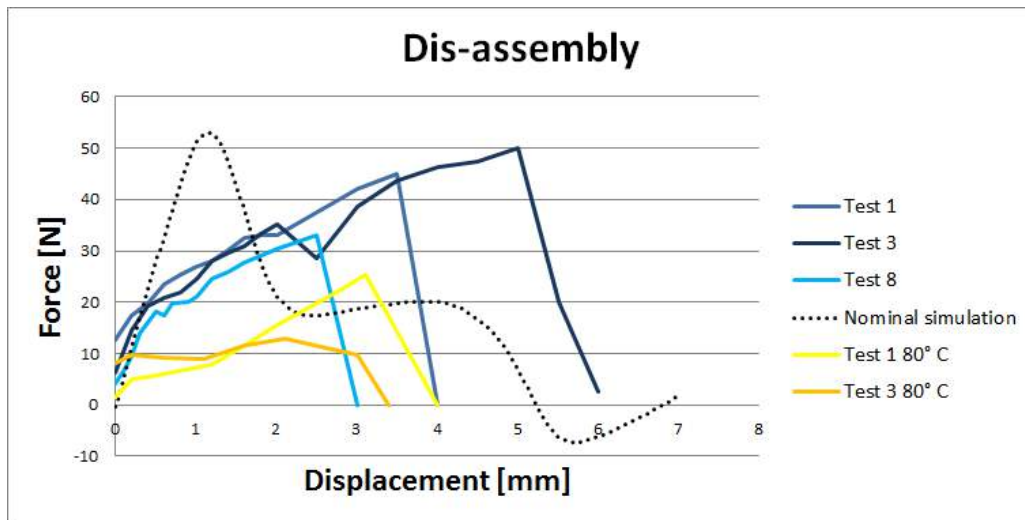Figure 4.1: *The assembly forces from tests and the detailed simulation model.*

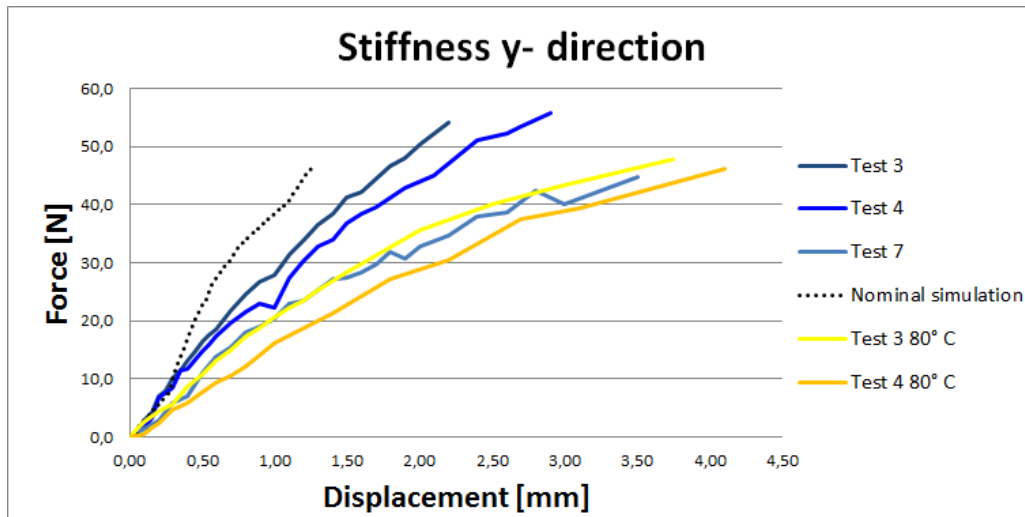Figure 4.2: *The force needed for dis-assembly at the tests.*

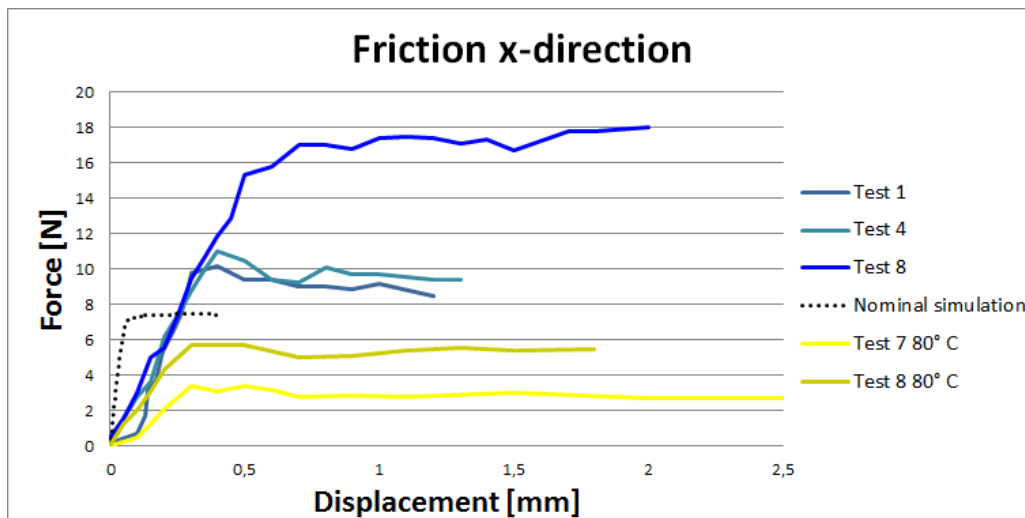Figure 4.3: *The force-displacement dependence in the y -direction.*

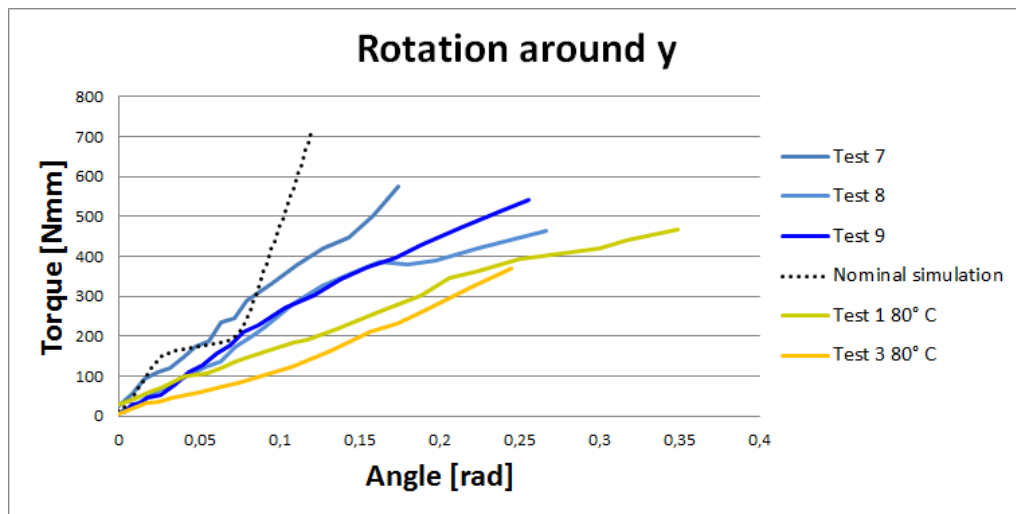Figure 4.4: *The friction tests at both room temperature and 80°C.*

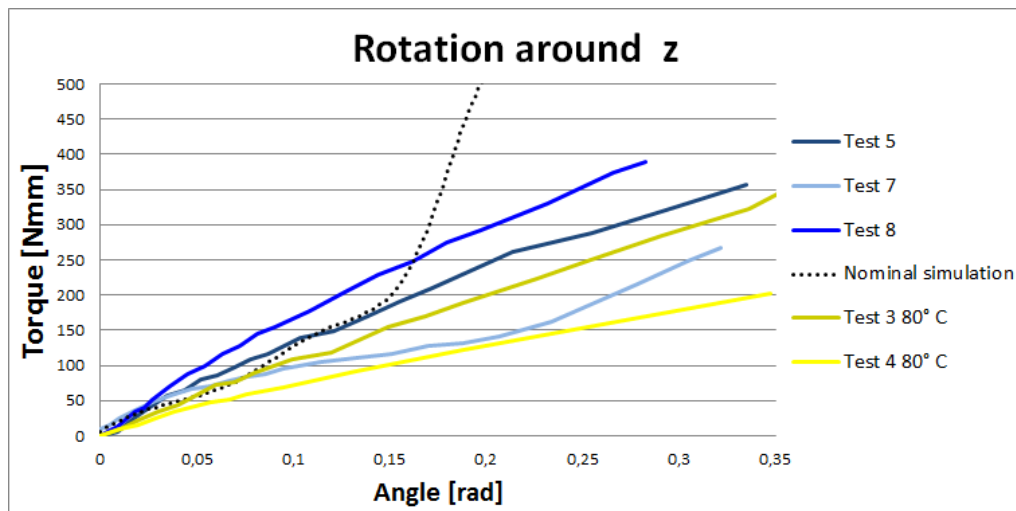Figure 4.5: *The measured torque verses applied angel of rotation around y-axis.*

Figure 4.6: *The measured torque versus applied angel of rotation around z-axis.*

4.1.1   Test to see influence of the plastic parts

In Figure 4.7 are the ordinary tests presented together with the tests to see the influence of the plastic part. This is the test with a added metal plate on the side. The tests with metal plate are ones heated and cooled and the hole is larger than the other at room temperature which is the reason to the lower friction force that more matches the tests at $80°C$.

4.1.2   Tests with different materials

The tests with different materials are shown in Appendix B. The friction behavior is also shown in Figure 4.8. The green graphs represent representative curves for the standard material combinations, ABS around the hole and PP at the tower. The blue is the different materials at room temperature and the yellow is at $80°C$.
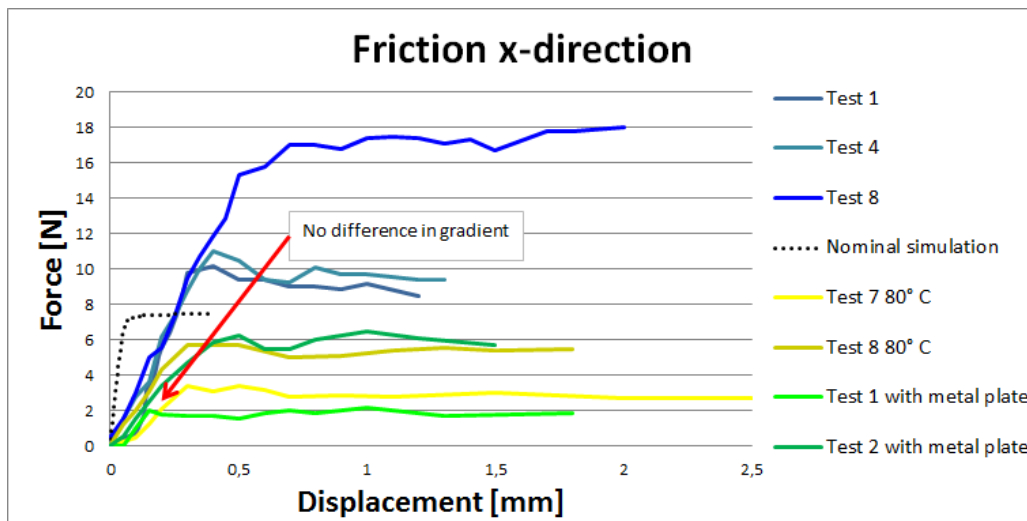
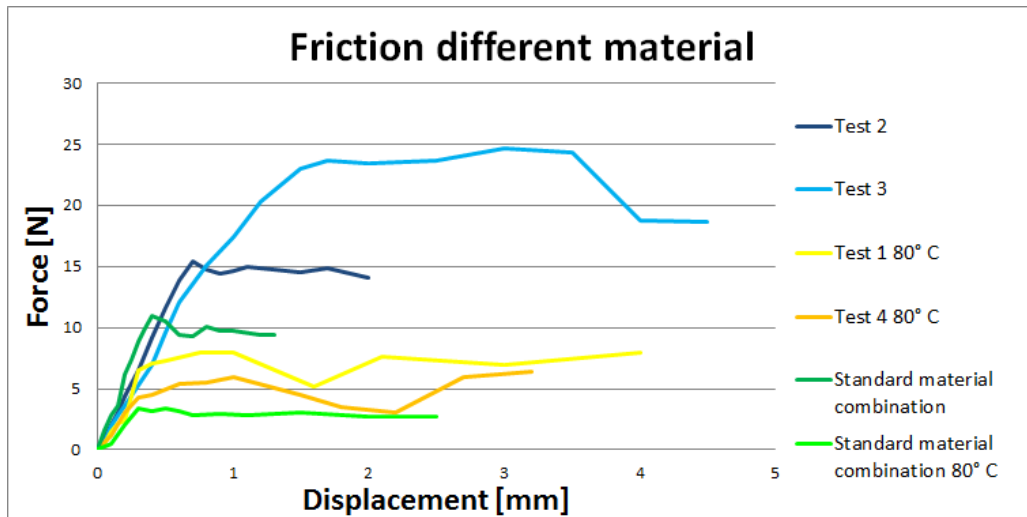Figure 4.7: *The performed tests to see plastic influence in friction.*

Figure 4.8: *Friction tests with different material combination.*

4.2 Numerical simulations

The FE-analysis gives a result that is noisy from the explicit solver. This noisy result is filtered so that the noise do not give any influence. The model with ABS around the hole and a PP tower gives the result for the total force that is needed under the assembly process as shown in Figure 4.9 at room temperature. The red line is the filtered result and the black is the unfiltered result.

The loaded assembled FEM-model in the x-direction gives a behavior as in Figure 4.10. This shows the friction force in the x-direction as the force at which the curve level out. In Figure 4.10 exist some stiffness in the beginning before the sliding between the clip and hole.

The force-displacement curve in the y-direction is not needed to be filtered due to that the noise is small in this simulation. The stiffness, k_y, is shown in Figure 4.11 as the gradient in the force vs displacement curve.
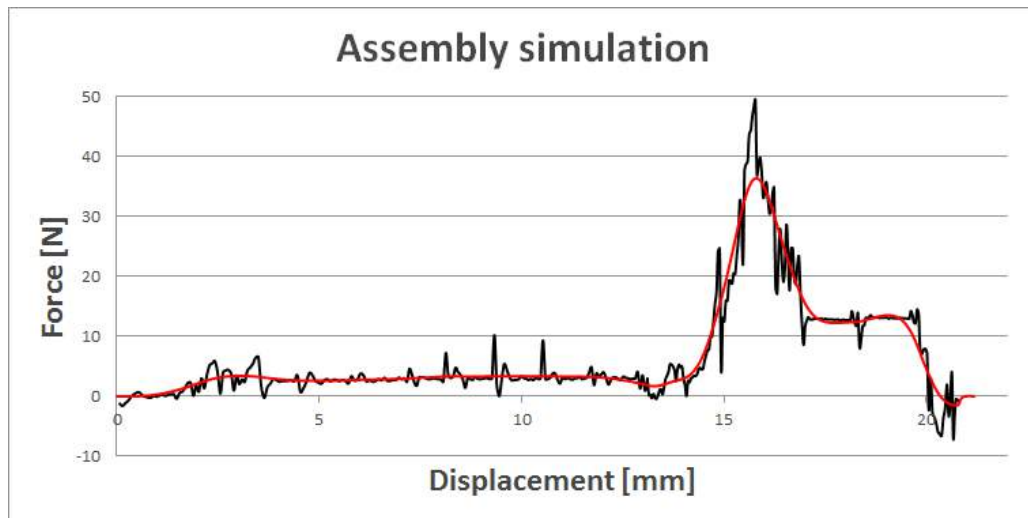
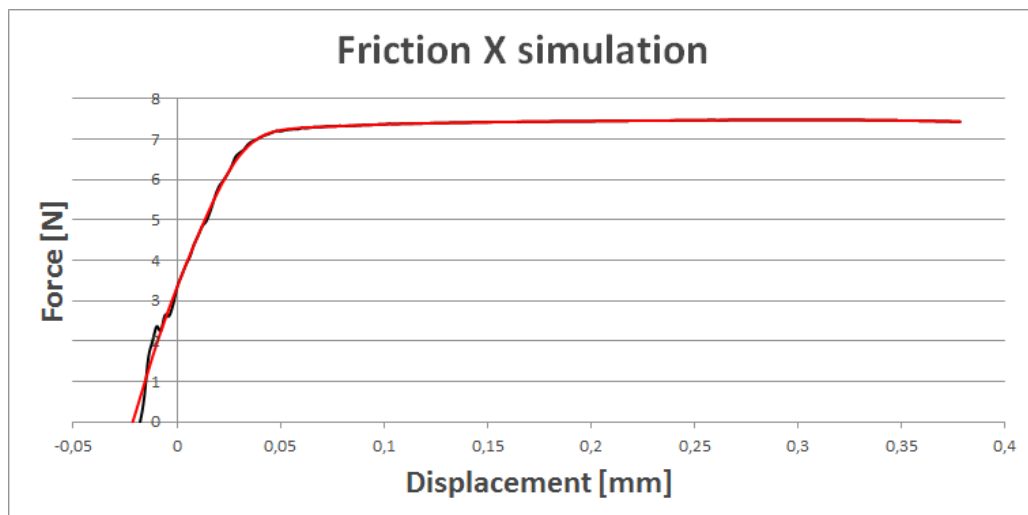Figure 4.9: *The assembly force over the displacement needed in the assembly.*

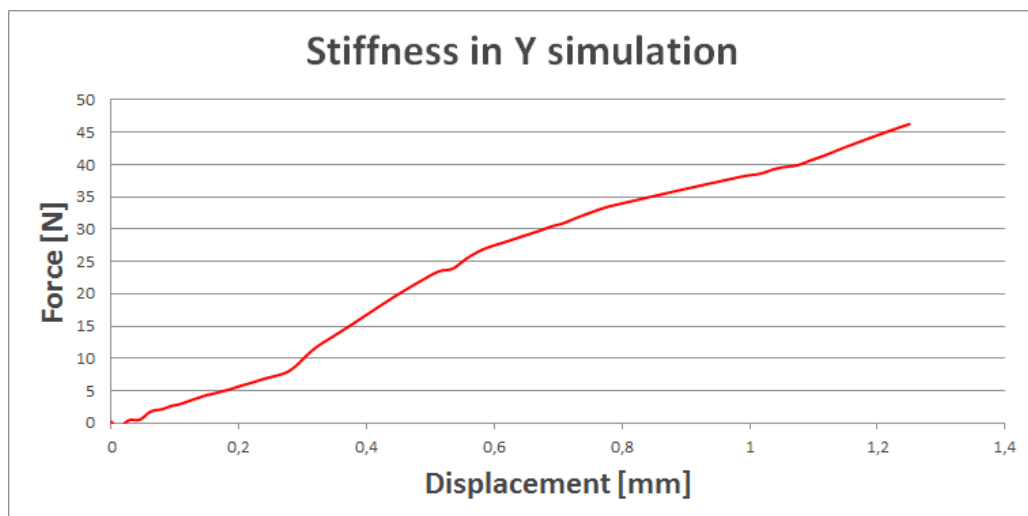Figure 4.10: *The force that is needed for the movement in friction.*

Figure 4.11: *The force vs displacement for movement in y-direction.*

The rotational stiffness, $k_{\phi y}$, around the y-axis from the simulation is the gradient in Figure 4.12. The curves are only valid until 0.08 *rad*. After this angle the clip deforming in an non trustful way.
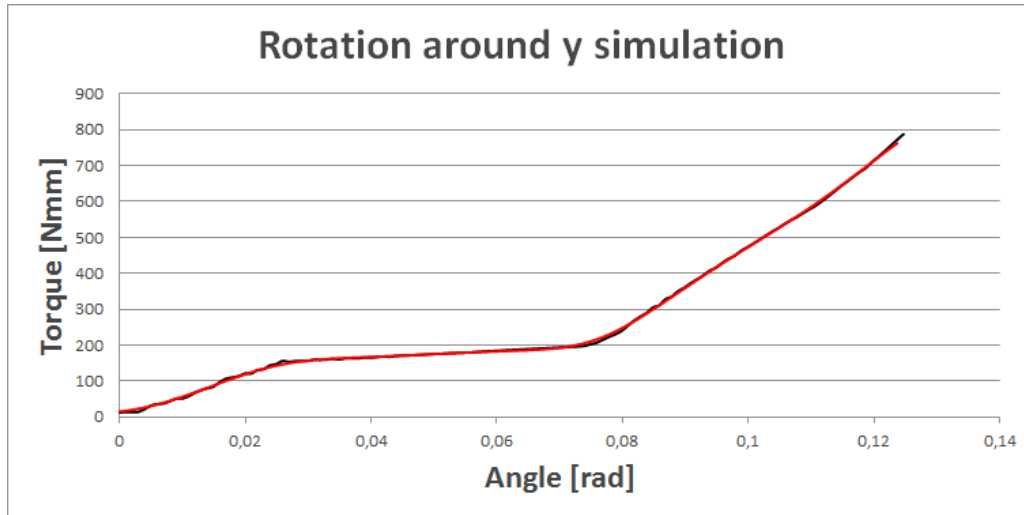

Figure 4.12: *The required torque to rotate the clip connection around the y-axis.*

The rotational stiffness around the z-axis, $k_{\phi z}$, is shown as the torque vs the rotational angle in Figure 4.13. The increase of the stiffness at the end of the simulation curve is due to that here comes the hole in contact with the tower and is deforming the tower.
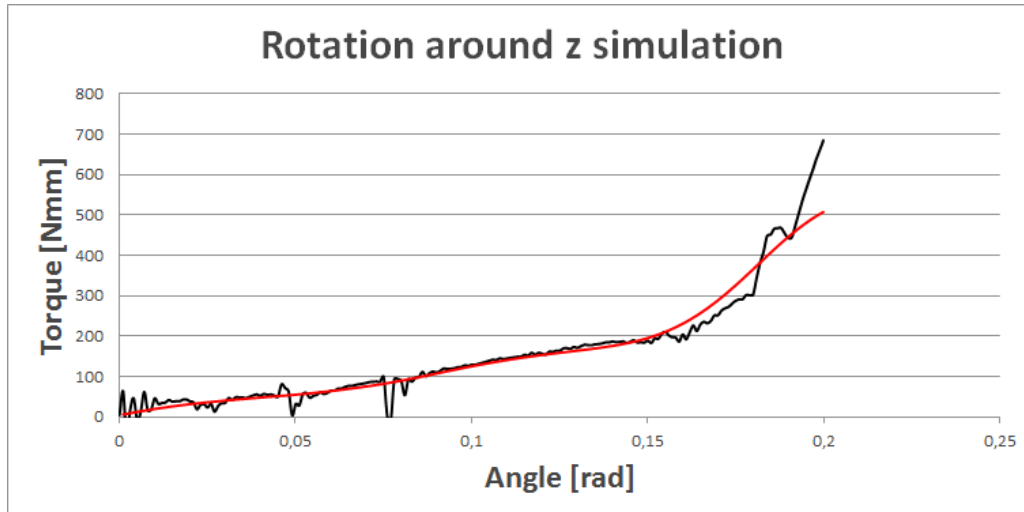

Figure 4.13: *The required torque to rotate the clip connection around the z-axis.*

To dis-assemble the clip connection is a force, F_{dis}, equivalent to the maximum in Figure 4.14 needed according to the FE-results for room temperature. This graph is similar to the second part of the assembly result in Figure 4.9 which is anticipated since the loading and behavior is similar.
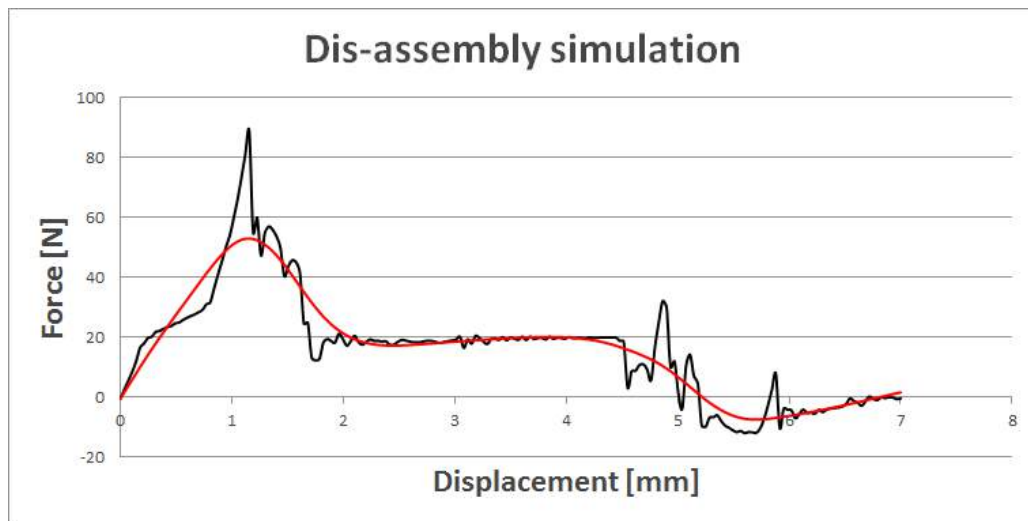
Figure 4.14: *The force that is required for the clip connection in the dis-assembly process.*

From the simulations it can be concluded that the deformation of the hole and tower is small and gives no big influence in the simulation result. From the simulations can not an exact value of the parameters be chosen since it depends on where in the graphs the calculation is performed. The parameter value is also sensitive to how the contact in some areas and how the boundary conditions are defined. This gives some difference in the results. Some difference comes also from how the simulation results are filtered.

4.2.1   Sensitivity analysis

The sensitivity analysis of the different parameters is shown in Figures 4.15-4.20. The black and grey line is the different simulations with variations of the nominal simulation such as e.g. finer mesh. The difference in Young's modulus at the clip is represented by the green lines. The blue lines represent the variations of the friction coefficients between the tower and the clip and the hole and the clip. All the yellow lines represents the variations of the clip thickness and the hole size. The moved clip and combination of the moved clip and tower is indicated by red in the figures. A table of the resulting approximate values in the sensitivity analysis are presented in Appendix G.

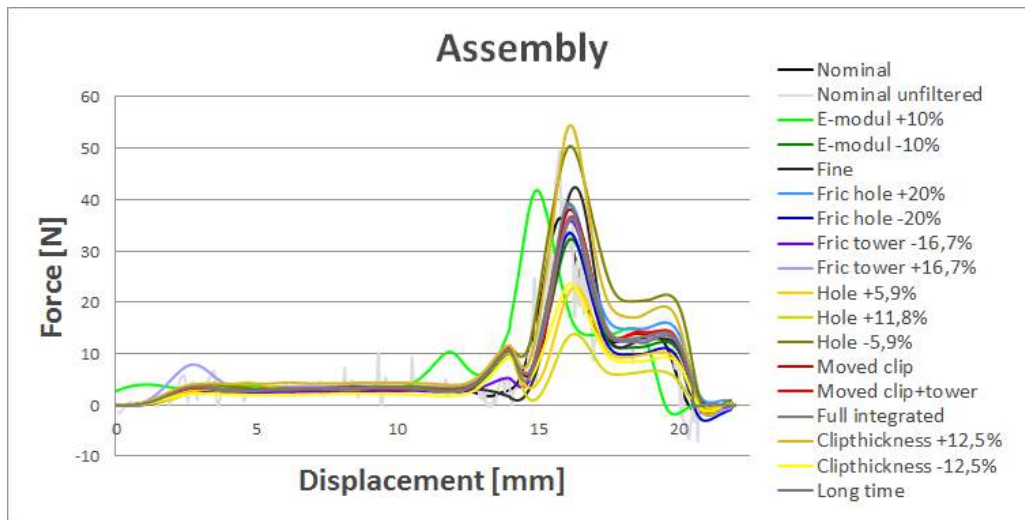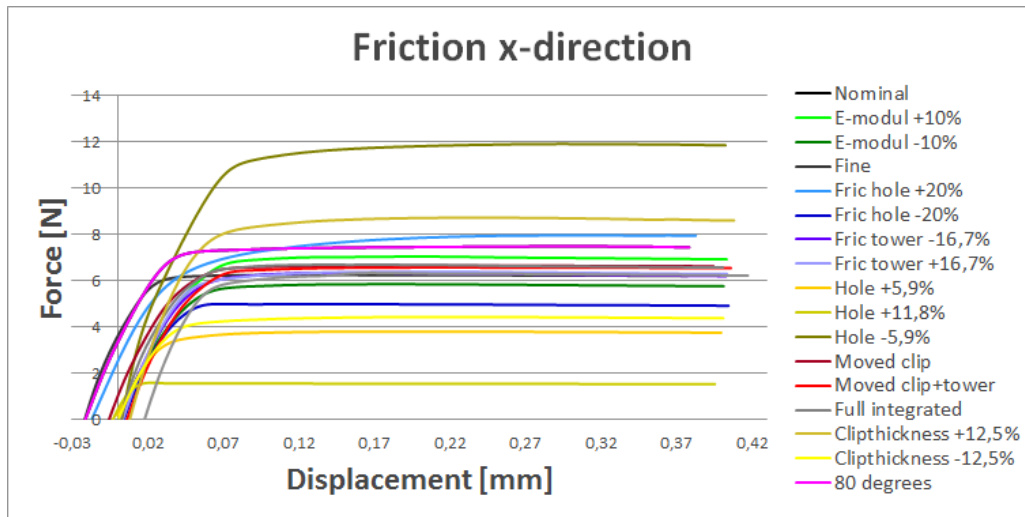Figure 4.15: *The sensitivity analysis of the assembly.*

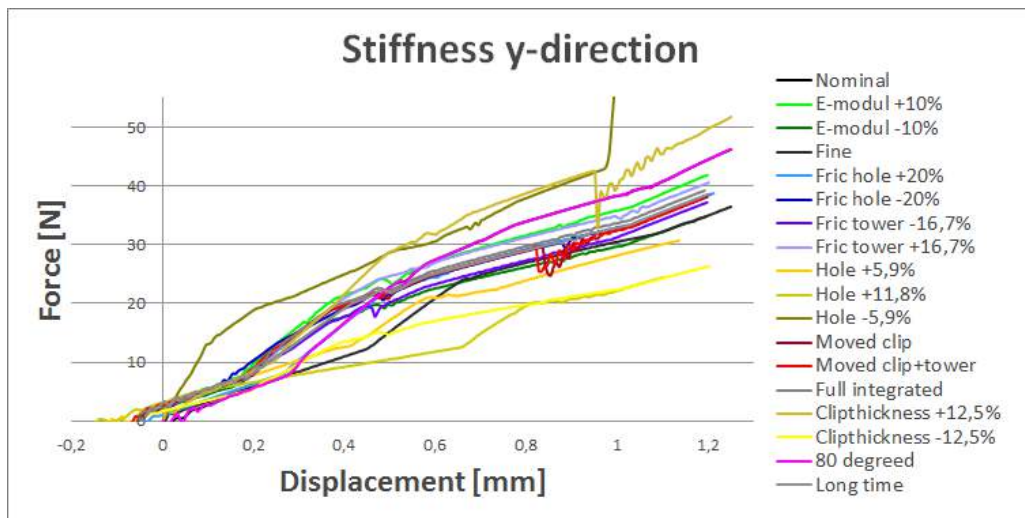Figure 4.16: *The sensitivity analysis of the friction in x-direction.*

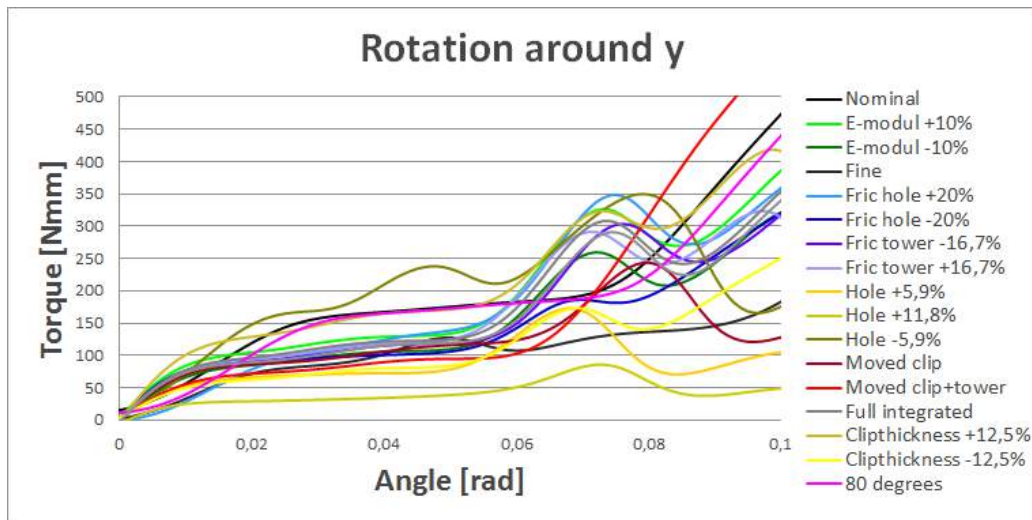Figure 4.17: *The sensitivity analysis of the stiffness in y-direction.*

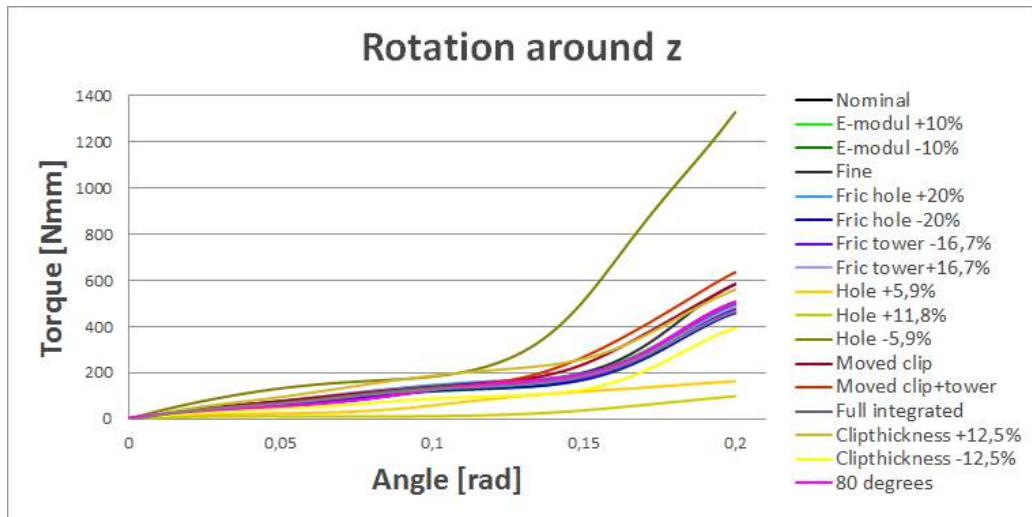Figure 4.18: *The sensitivity analysis of the rotation around y-axis.*

Figure 4.19: *The sensitivity analysis of the rotation around z-axis.*
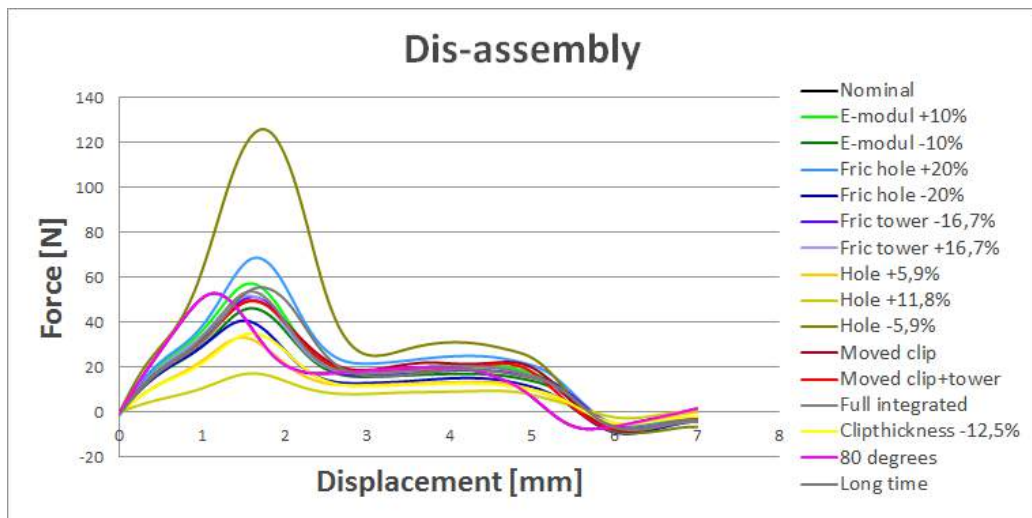
Figure 4.20: *The sensitivity analysis of the dis-assembly.*

4.3 Calibration

In this section the chosen values of the properties are presented. For a more detailed discussion on how the suggested and implemented values are selected see Section 5.4. The overall strategy when selecting the parameters is to compare the tests with the simulations. The weight between this to is done with influence of the tolerances of the parts, the error sources and the values in the sensitivity analysis. At the end the comparison is done from the sense of what gives the best reliable result.

The assembly force is not implemented in the connector element of the clip but is still evaluated. From looking at the tests of the assembly force it is concluded that a reasonable value of the required assembly force is $F_{ass} = 38\ N$, see Figure 4.21. This value is also close to the value from the simulation. A stop in the positive z-direction is implemented in the simple model to prevent any movement of the clip in this direction.

Figure 4.21: *Suggested assembly force together with the tests and simulation.*

Figure 4.22: *The suggested behavior in x-direction at both room temperature and* 80°.

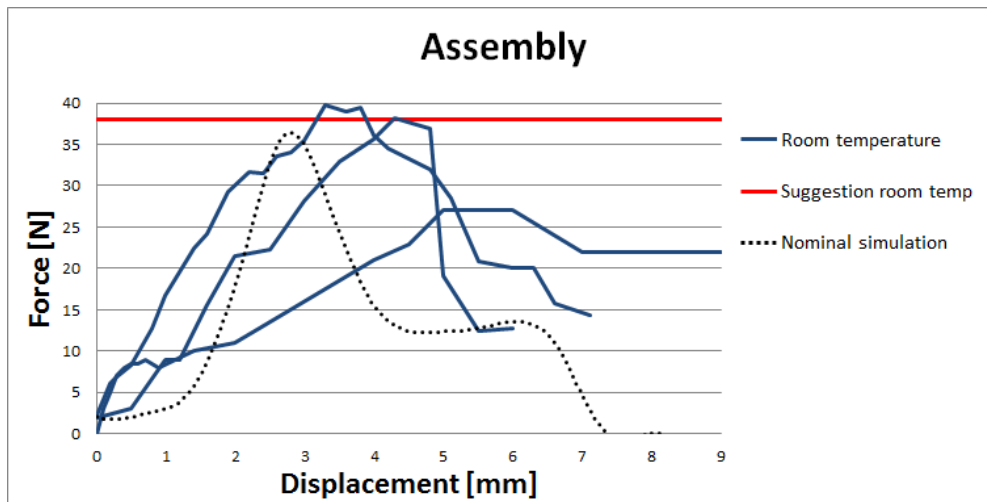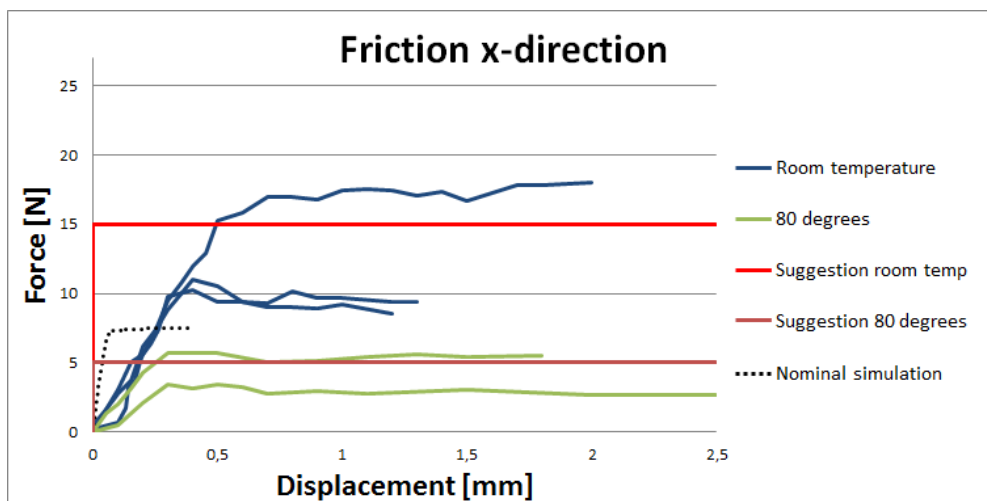The selected value of the required force for sliding in x-direction at room temperature is set to $F_f = 15\ N$. A stick stiffness is not implemented in the model. The friction force is implemented to be independent of the normal force due to that the pretension in the clip joint is unknown. At $80°C$ is instead a sliding force of $F_f = 5\ N$ implemented. The implemented values are presented in Figure 4.22. The selected value are based on the test due to the uncertainties of the friction coefficient in the simulations. The chosen values are set higher than the average tests to be conservative in the intended application. The clip joint can only move $2\ mm$ in the x-direction before the tower hits the hole. At this displacement is a stop added.

The stiffness in the y-direction is assumed to be linear with the value $k_y = 32\ N/mm$. This value is based on the simulation due to that this is assumed to be more trustful. A higher stiffness is also conservative in the intended application. To assume linearity is simple and matches the tests and simulation good even if non is linear, see Figure 4.23. At $80°C$ the stiffness is assumed to be $k_y = 22.5\ N/mm$. The presented values are only valid until a displacement of $1.2\ mm$ is reached. At this displacement a stop is added to represent that the tower comes in contact with the hole.
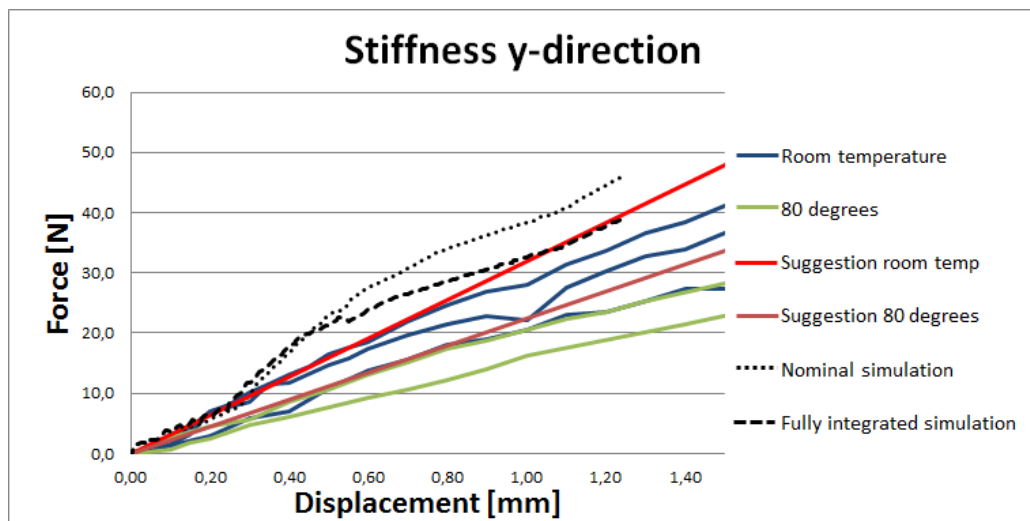
Figure 4.23: *Graph of the suggested stiffnesses in y-direction with tests and simulations.*
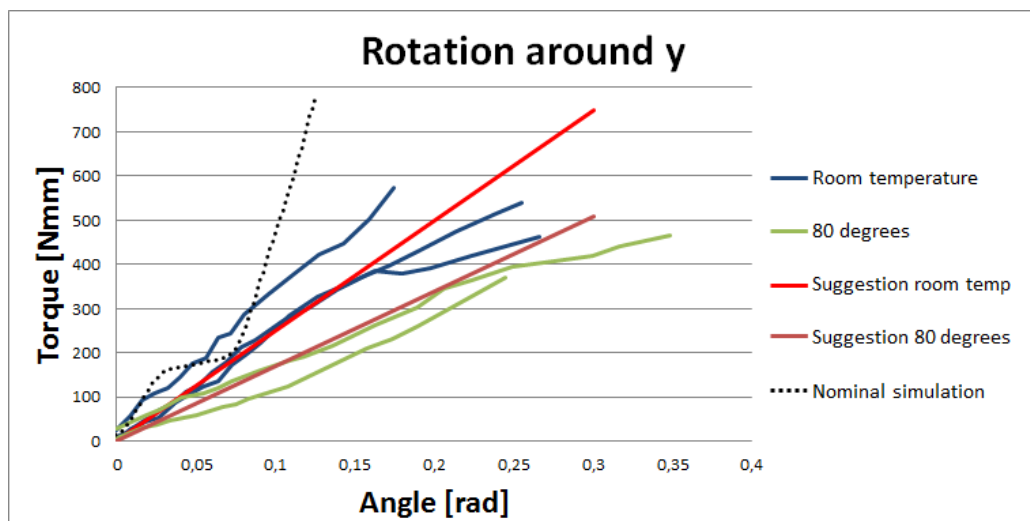
Figure 4.24: *Suggested stiffness and the tests and simulation around the y-axis.*

The rotational stiffness around the y-axis is based on the tests rather than the simulation. The value is set to $k_{\phi y} = 2500 \ Nmm/rad$ at room temperature and $k_{\phi y} = 1700 \ Nmm/rad$ at 80°C. This linear stiffness matches the tests in a good way, see Figure 4.24. The simulation gives that a stop is implemented at 0.08 rad due to that here is a big increase in the stiffness from doubtful behavior of the clip.

The average curve of the tests matches the simulation curve well in rotation around the z-axis. It is assumed that the stiffness does not change with the temperature based on the tests. The value of the rotational stiffness is chosen to be $k_{\phi z} = 1250 \ Nmm/rad$, see Figure 4.25. From the geometry of the clip connection it is concluded that the maximum angle of rotation possible in the clip joint is 0.15 rad.
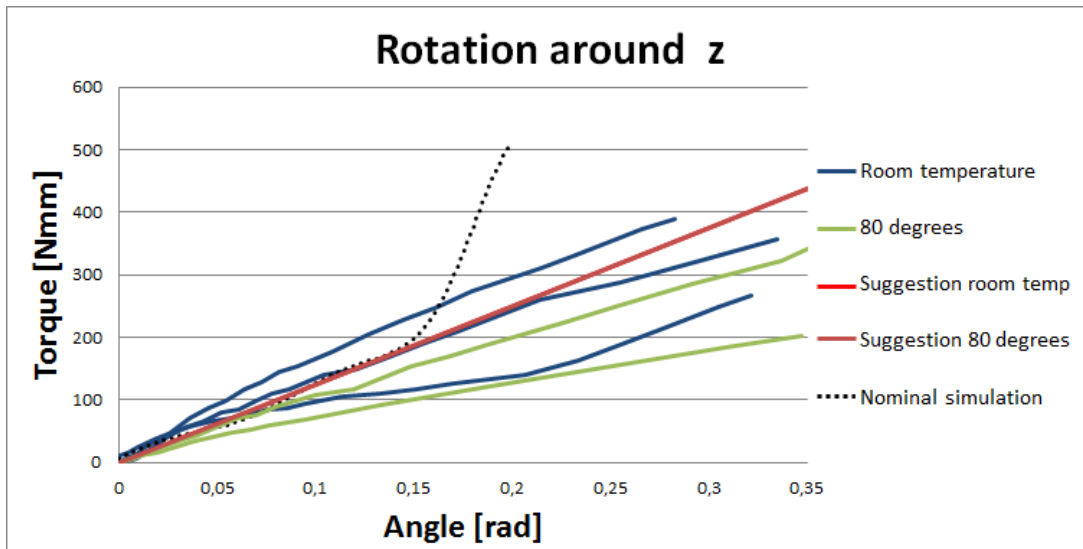
Figure 4.25: *Tests together with the simulation and the suggested stiffness.*
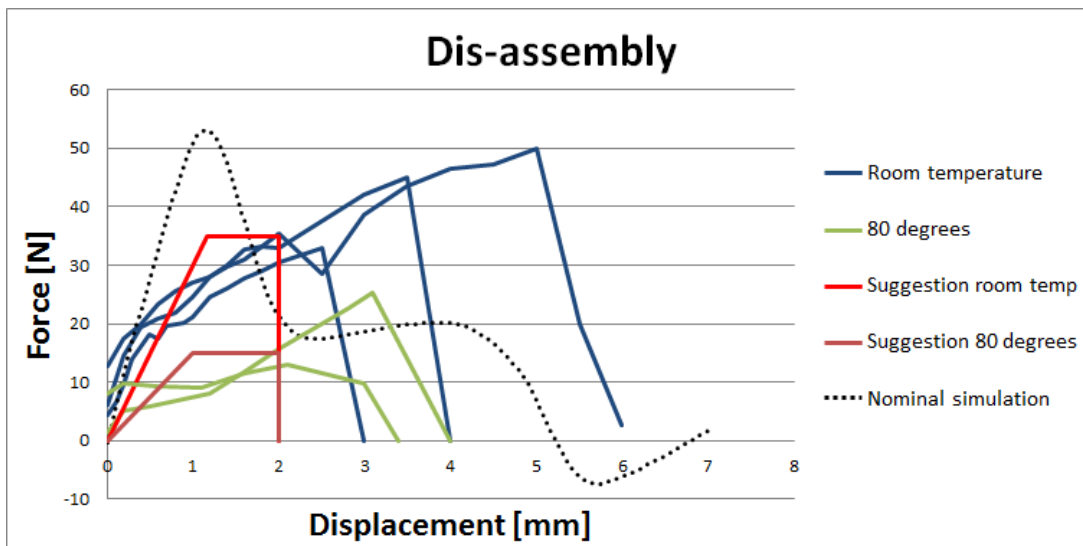
Figure 4.26: *The suggested behavior in the -z-direction together with the results from tests and simulation.*

The motion of the clip in the negative z-direction is assumed in the simplified model to have a stiffness of $k_t = 30\ N/mm$. When the force in this direction have reached $F_{dis} = 35\ N$ the clip joint is assumed to slide until the displacement $2\ mm$ with this force and then break, see Figure 4.26. The same behavior is assumed for $80°C$ but with $k_t = 15\ N/mm$, $F_{dis} = 15\ N$ and a total displacement of $2\ mm$. The required force of dis-assembly is set lower than the average test and simulation to be on the conservative side.

A value $4000\ Nmm/rad$ is implemented as a rotational stiffness around the x-axis for the connector element according to the simple study presented in Appendix F. A stop is also added at an angle of $0.08\ rad$. These values are assumed to be valid also for $80°C$.

The constructed connector element is with the implemented values checked to give the expected behavior in all directions under specific forces.

5 Discussion

The results obtained in the presented thesis work may be used in the simulations of parts at Volvo Cars. Even if the study cannot conclude an exact behavior of the clip joint it gives a more advanced element to represent the clip connection than the current one in use. The properties of the clip joint can be determined to an approximate value. A more detailed discussion about the different part of the study is presented below.

5.1 Discussion about the tests

The physical test results for the majority of parameters do not show much deviation. The deviation is greatest for the rotational stiffness around the y-axis but can still be used to draw a conclusion about the stiffness. In the friction tests the friction force appear to be collected at two different values at each temperature. These two levels are not far from one another and an approximate value is easy to observe at both temperatures. When comparing to the previous measurements, see Appendix A, it can be concluded that the problem with the clip getting stuck in friction testing cannot be seen in this test. The stiffness around y-axis was also tested in previous tests but gets larger in this study. This can be due to somewhat different test setups and that the there is a spread and the one tested before can be in the lower range.

When evaluating the tests and trying to find out if there is any clear relation between the tests that gives divergent result is not any found. For some parameters indeed the same tested clip gives divergent result at both room temperature and at $80°C$. For example is the test that gives low values in Figure 4.2 at both room temperature and $80°C$ performed using the same clip. The reason for the discrepancy can be both that there is something that went wrong when testing the clips or that the clip has a divergent property. The small dependence that can be seen between individual clips and divergent results is only valid for individual parameters and not all parameters.

Some of the tests in room temperature were performed the same day as the assembly was done and some were performed when the clips had been assembled for one week. No measurements of how this effect the deformation of the clip and hole was done. When comparing the different tests can no clear difference be seen between the one tested directly and the ones assembled for a week but some dependence can still exist. Normally is there creep in the material that e.g. can increase the hole size with the time.

From the measurement of the hole size it is concluded that the difference in hole size is small and that the difference in test results depending on the hole size is not big enough to draw any conclusion since the variation between all test is bigger than between the differences in hole sizes. The measurement of the hole size was difficult to get precisely which makes it possible that the dependence shown in the sensitivity analysis still can exist.

From the result in Figure 4.8 can be seen that when changing the materials is the properties changed somewhat and the material have some influence. But most likely are the properties of the clip joint more depending on the geometry of the clip connection than the properties of the materials. It is also concluded from the sensitivity analysis that the normal forces at equilibrium are more important than the friction coefficients, see Section 5.3. The conclusion that the materials does not influence the results is only based on the few tests with PP around the hole and ABS at tower. Changes may happen for other materials.

5.1.1 Error sources

In the test some general error sources can be found. One of the errors might be in the readout of the displacement and force since there was a small delay of the display of the force from the applied displacement. The force that is read is also an average over a small time.

One big issue in the tests is to exclude the influence of the hole and tower from the clip joint. In reality is everything between coordinate table and the attachment of the vise in the table included in the measurement. One dependence is that the tower and hole can come in contact and this dependence is unwanted. When the component is heated before the tests at $80°C$ the hole size is changed and it gets a little bit bigger. When whole parts is used it is likely that the hole does not get that much larger at heating. Testing at a bigger part gives some other problems, e.g. to center the load in friction, and this is not recommended from that point of view.

The deformation of the plastic parts can also give other influences on the test results. One of them is that it is possible that at the beginning of the loading the plastic at the tip of the force sensor is deformed and gives some additional stiffness. This together with that the edge of the hole can deform and create a stiffness, see Figure 5.1, might be the reason of the stiffness in x-direction before sliding. But the tests done with reinforcement of metal plate on the side speak against this since the stiffness still exist, see Figure 4.7. The same mechanism can also have some influence on the stiffness in y-direction even if it most likely is smaller due to that the clips holds back from the other side of the loading.
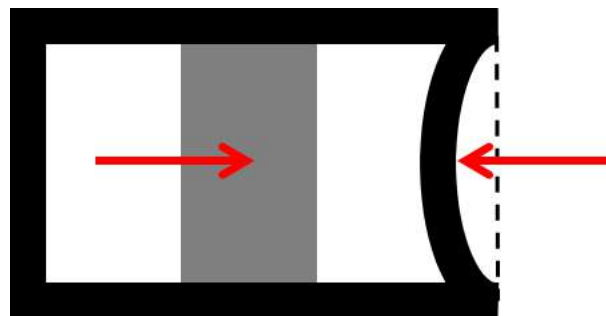

Figure 5.1: *Sketch of the influence of the edge deformation.*

It might be possible that the test piece moves in the vise and that this gives some influence in the measured stiffnesses. In the assembly and dis-assembly there can also be some movement in the metal and between the metal and the hole.

In the tests of the rotational stiffnesses is the problem primarily that with the available equipment it was not possible to have a centered force with the same magnitude at the opposite side during loading, see Figure 2.2. This causes the translational stiffness to have a small influence on the result.
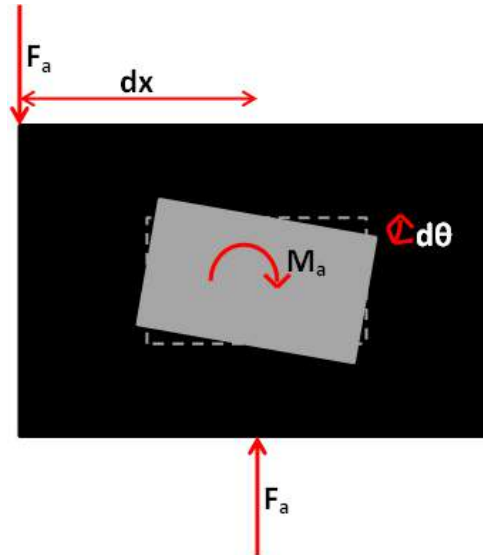

Figure 2.2: *Illustration of equilibrium of a clip joint loaded with a torque. (repeated from page 8)*

The tests at $80°C$ may not be at exactly $80°C$ since the test pieces was heated to $90°C$ and the tests performed in room temperature. The 1-2 minutes until the tests was finalized can make the temperature to be smaller or larger than $80°C$. The temperature varies probably also under the test and this can effect the result.

5.2 Discussion about simulations

In the simulations is a stiff hole used to minimize the influence from the hole on the properties. Even in the simulation for $80°C$ is the hole hold still and is stiffened so that the hole does not expand. This is done because that in reality is the hole in a surrounding part and the surrounding part prevents the hole from expanding free. The hole might expand more than in the simulations. The expansion of the hole can also be different in reality at different areas of the parts.

The explicit solution procedure tends to give a noisy result which need some type of filtering. The filtering of the result should capture the behavior as good as possible without the noise. This is sometimes hard and therefore should the outcome from the simulations not be taken as being specific but rather as approximations. How the contacts and the boundary conditions are defined gives also a variation in the result. For example in the dis-assembly loading with constraints in all the directions except z direction gives a lower dis-assembly force than if it is free in the other directions. To be conservative the only possible motion in z is chosen. Because of this difference it is also investigated if a difference happens if a loading on top or at the bottom of the tower is used, see Appendix C. It is concluded that the different loading's gives almost the same result.

In the assembly process shown in Figure 4.9 can be seen that in the first part of the curve up to approximately 14 *mm* a small force is needed to assemble the clip to the tower. In the following peak a larger force is needed to get the clips flanges to enter the hole and then at the flat surface the clip slides in the hole. In the friction curve, see Figure 4.10, can a high stiffness be seen in the first part. This is probably due to some deformation of the clip and this can also be seen in the energies, see Appendix E. Some of the stiffness can also come from the contact modeling method, see Section 2.3.2. The next part of the curve when the force level out at a certain value represents the sliding.

The stiffness in the y-direction, see the gradient in Figure 4.11, is almost constant the hole time. The small changes is due to new contact areas between the clip and the hole. For the rotational stiffness around the y-axis, see Figure 4.12, the first small change in gradient is due to that the friction between the hole and clip changes from the loading. The next change is due to that the clip in the simulations deforms in an unrealistic way due to a large rotation.

In Figure 4.13 of the rotational stiffness around the z-axis is the stiffness almost constant up to 0.15 *rad* where a big change happens. The big change is due to that the hole and tower comes in contact. The behavior in dis-assembly simulation, see Figure 4.14, is the similar to the last part of the assembly process. This is due to that also here the flanges are first compressed to fit in the hole and then the sliding in friction occurs inside the hole.

The behavior in the simulations can also be explained to some extend with what happens in the energies. This is explained in Appendix E. For example can in the dis-assembly process be seen that under the hole process needs some energy be added to overcome the friction. In the beginning also energy is needed to compress the flanges and this is stored as strain energy in the clip until the flanges passes the end of the hole and the strain energy is released.

5.3 Discussion about sensitivity analysis

From the sensitivity analysis it can be concluded that the most important parameter is the hole size and the thickness of the clip. A modification of the hole size or the clip thickness gives a change in all of the parameters and is even more important to the friction than the friction coefficient, see Figure 4.16. The importance on the friction is probably because that the hole size and clip thickness gives a big difference in the normal force between the hole and the clip and in that way influence the friction force. The difference in normal force has also to do with at what place the clip joint find the static equilibrium. The chosen values in the sensitivity analysis are greater than the tolerances to clearly see the differences this gives in the properties of the clip. In the future it is recommended to investigate what difference a changed thickness of the tower gives on the properties.

In the analysis of the dis-assembly force has not a result for the fine mesh and the thicker clip been reported due to numerical issues. In these analysis there was more problem with the contact and friction than in the other simulations. The problem was that the hole and clip get stuck to each other and that the force to dis-assemble the clip gets unreasonable high. To avoid this it was tested to exclude the friction but then the result of the dis-assembly force gets too low and is not comparable to other simulations. See Appendix D for example of the result for the thicker clip.

The numerical problem that appears in the dis-assembly analyse for thicker clip can be explained by observing the energies in the analysis. The reaction force is shown together with the different energies in Appendix D.1. From this it can be concluded that when the force goes beyond the reasonable values is the internal energy in the clip joint also increasing drastically in the form of strain energy. This fits well with the observed behavior that the clip deforms in an unreasonable way when the contact gets stuck. When the contact finally starts sliding is the stored energy released as frictional dissipation. The described problem with the contact is only seen in the dis-assembly simulations with fine mesh and thick clip. For example it can not be seen in the nominal simulation, see Appendix E.

In the sensitivity analysis of the assembly a small peak can be seen before the big peak, see Figure 4.15. This small peak is nothing real and is only based on that there happens a energy release between loading to assemble the clip on the tower and assemble the clip in the hole.

5.4 Discussion about calibration

All the parameters in the constructed connector element is set to be independent on each other and only dependent on the temperature. The simulations with $80°C$ is not considered since the values isn't believable. If the hole wasn't constrained would it give an increase in hole size and this is investigated in the sensitivity analysis.

The stops is added when the tower and hole is in contact because then the behavior from the parts dominates the response and the stiffness from the clip is small in comparison. With the stop the connection starts to act as a rigid connection in that direction after a set displacement. Since the connection is fastened into the different parts with spiders, see Section 1.1.4 and 3.2.3, is the parts deformed when the connector element act like a rigid element. With the present implemented connector element is no contact needed between the parts to investigate when the tower and hole is in contact and the simulation time can be minimized.

The assembly force is taken as an estimated average of the results from tests and simulations, see Figure 4.21. The stiffness in the x-direction is not implemented due to that the reason for the stiffness not can be established. Therefore it is more conservative to exclude this. To have conservative values of the friction force is a value larger than the average used, see Figure 4.22. The value from the simulation is not taken into account much due to the uncertain friction coefficient and hole size. The friction force implemented is set to be independent on the loading in the y-direction. The friction behavior is implemented as elasticity which makes the clip to go back to the original position when unloaded. To return to the original position is not representative of the reality.

The value of the stiffness in the y-direction is in room temperature mostly based on the simulation result. The result from simulation is higher than the results from tests and a higher stiffness is more conservative. The chosen value from the simulation is not taken from the nominal simulation since it can be a to high stiffness in this simulation. The chosen value is based on the simulation with fully integrated elements in the sensitivity analysis. This is based on that the fully integrated, the nominal, the fine mesh and the longer time simulations should give approximately the same stiffness. The fully integrated simulations is chosen since it gives the value that is the median. The value of the stiffness in y-direction for $80°C$ is selected to be the same percentage lower as the difference is in the tests between the different temperatures, see Figure 4.23.

When looking at results for the rotational stiffness around y-axis it can be seen that the tests and simulation matches well up to the stop at 0.08 rad, see Figure 4.24. The selected value of stiffness is taken from a combination of tests and simulations. For higher temperature it can be seen that the stiffness goes down in the tests and this stiffness is also selected with a smaller value.

The simulation and average of the tests at room temperature gives approximately the same value of the rotational stiffness around the z-axis and this value is also chosen, see Figure 4.25. The stiffness around the z-axis at $80°C$ is close to the stiffness at room temperature in the tests. Based on this is the chosen stiffness selected to be constant with the temperature. The rotational stiffness around the x-axis is not studied in detail and is based on an assumption of being constant with the temperature.

In the dis-assembly direction is a corresponding stiffness that is close to the simulation results in the sensitivity analysis chosen. The stiffness in the nominal simulation is not chosen since it is larger than the other in the sensitivity analysis. The force for dis-assembly is selected in the lower range from the tests to be conservative, see Figure 4.26. The displacement of release is also set in the lower range to be conservative.

5.5 Conclusion

In Table 5.1 is the selected values for the properties to implement in the connector element presented in the coordinate system presented in Figure 1.6. These values represent the clip connection in a good way and the connector element is still a simple representation of the clip. The values are chosen to be conservative for the intended application. With the created connector element is the purpose of the thesis fulfilled.

The implemented properties is approximate and can not be taken as an exact value. The most important parameters in the clip joint that is evaluated according to the results from the sensitivity analysis are the thickness of the clip and the width of the hole.

Table 5.1: Summary of the implemented values for the properties of the proposed connector element.

| Parameter	Maximum movement room temperature	Maximum movement 80°C	Stiffness/Force room temperature	Stiffness/Force 80°C
Friction in x	$\pm 2\ mm$	$\pm 2\ mm$	Sliding at 15 N	Sliding at 5 N
Stiffness in y	$\pm 1.2\ mm$	$\pm 1.2\ mm$	32 N/mm	22.5 N/mm
Assembly force	-	-	38 N	-
Stiffness in z	0	0	-	-
Stiffness in -z	1.17 mm	1 mm	30 N/mm	15 N/mm
Dis-assembly force	0.83 mm	1 mm	35 N	15 N
Rotational stiffness around x	$\pm 0.08\ rad$	$\pm 0.08\ rad$	4000 Nmm/rad	4000 Nmm/rad
Rotational stiffness around y	$\pm 0.08\ rad$	$\pm 0.08 rad$	2500 Nmm/rad	1700 Nmm/rad
Rotational stiffness around z	$\pm 0.15\ rad$	$\pm 0.15\ rad$	1250 Nmm/rad	1250 Nmm/rad
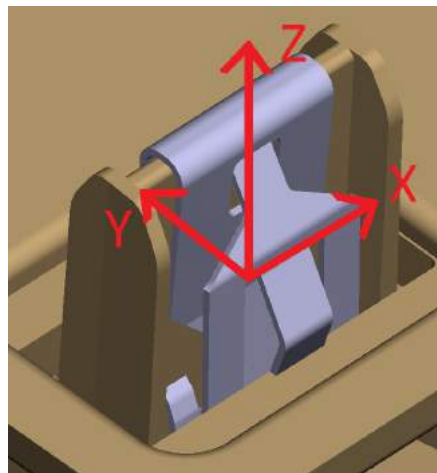
Figure 1.6: *The definition of the coordinate system of the clip joint. (repeated from page 4)*

6 Future Work

In the future to get a more accurate model of the clip joint it is recommended to investigate some properties of the clip closer. One of them is to validate the rotational stiffness around the x-axis with some tests and not only base the result on simulation.

The investigation on other materials might need to be more comprehensive and also include other possible material combinations to ensure that the parameters are valid. To have an even higher accuracy of the parameters can the test be repeated with a higher resolution and a test setup that minimize the error sources more. For example may the tests be performed inside a climate chamber to control the temperature in a better way. It might also be of interest to have more material left at some tests to make the hole deform less at heating. In the future it is also recommended to investigate what difference a thickness change of the tower makes as a part of the sensitivity analysis.

An extended investigation on how the creep and relaxation in the materials might affect the results is suggested. It is also suggested to go more in to detail in the contact and friction formulations in the simulations. To have a better contact and friction formulation might give a higher resolution on the results.

To achieve a more accurate behavior in the connector element can for example the stiffness seen in x-direction and non linear stiffnesses in all directions be implemented. If this stiffnesses will be implemented is it recommended to investigate the behavior further. It is recommended in the future to change the frictional behavior in the connector element from implemented as elasticity to be implemented so that the clip does not return to the original position at unloading.

In an extended study of this clip connection could it also be of interest to look at the inter-dependency between the parameters in the joint. For example can the friction in x-direction depend on the displacement in y-direction. This might be the case due to that when loading the clip joint in y-direction is the normal force between the hole and the clip changed and thereby can also the friction force change.

References

[1] BETA CAE Systems SA. *Ansa*. Version 16.1.0. 2017.

[2] A. Korolija. "FE-modeling of bolted joints in structures". MA thesis. Linköping University department of Mechanical Engineering, 2012.

[3] A. Ugural and S. Fenster. *Strength and applied elasticity*. 4th ed. Prentice Hall, 2003. ISBN: 0-13-047392-8.

[4] R. Grahn and P.-Å. Jansson. *Mekanik*. Studentlitteratur, 2011. ISBN: 978-91-44-01909-3.

[5] Dassault Systèmes. *Abaqus Theory Guide. Coulomb friction*. Version 6.14. 2017. URL: `http://se-got-fs02:2080/v6.14/books/stm/default.htm?startat=ch05s02ath137.html`.

[6] P. J. Blau. *ASM Handbook. Appendix: Static and Kinetic Friction Coefficients for Selected Materials*. Vol. 18. 1992. ISBN: 0-87170-380-7. URL: `http://products.asminternational.org.proxy.lib.chalmers.se/hbk/index.jsp`.

[7] H. Petersson and N. Saabye Ottosen. *Introduction to the finite element method*. Prentice Hall, 2006, pp. 253–254, 292–306. ISBN: 978-0-13-473877-2.

[8] Dassault Systèmes. *Abaqus Theory Guide. Isotropic elasto-plasticity*. Version 6.14. 2017. URL: `http://se-got-fs02:2080/v6.14/books/stm/default.htm?startat=ch04s03ath104.html`.

[9] Dassault Systèmes. *Abaqus Theory Guide. Explicit dynamic analysis*. Version 6.14. 2017. URL: `http://se-got-fs02:2080/v6.14/books/stm/default.htm?startat=ch02s04ath23.html`.

[10] B. Sundström. *Handbok och formelsamling i Hållfastighetslära*. 7th ed. Instutitionen för hållfasthetslära KTH, 2010.

[11] P. Wriggers. *Nonlinear Finite Element Methods*. Springer, 2008, pp. 82–212. ISBN: 978-3-540-71000-4.

[12] R. Craig and A. Kurdila. *Fundamentals of Structural Dynamics*. 2nd ed. John Wiley & Sons Inc., 2006. ISBN: 978-0-471-43044-5.

[13] R. Cook, D. Malkus, and M. Plesha. *Concepts and Applications of Finite Element Analysis*. 3rd ed. John Wiley & Sons Inc., 1989. ISBN: 0-471-84788-7.

[14] P. Wriggers. *Computational Contact Mechanics*. Second Edition. Springer, 2006, pp. 15–16, 328–337. ISBN: 978-3-540-32608-3.

[15] J. Hetherington. "The Bipenalty Method for Explicit Structural Dynamics". PhD thesis. University of Sheffield Department of Civil and Structural Engineering, 2014.

[16] Dassault Systèmes. *Abaqus Analysis User's Guide. Connector Elements*. Version 6.14. 2017. URL: `http://se-got-fs02:2080/v6.14/books/usb/default.htm?startat=pt06ch31.html`.

[17] N. Instruments. *Dasylab*. 2013.

[18] Dassault Systèmes. *Abaqus Analysis User's Guide. Coupling constraints*. Version 6.14. 2017. URL: `http://se-got-fs02:2080/v6.14/books/usb/default.htm?startat=pt08ch35s03aus133.html`.

[19] Volvo Car Corporation. *Sliding attachments in strength analysis*. 2016.

Appendices

A   Previous measurements

The simple measurement that was done at Volvo Cars is presented in Table A.1. The performed tests had large variation in friction and only one test was done for the rotational stiffness around y. The spread happens due to that the clip dug in to the plastic at the inner side of the hole. These two parameters where the only tested. The other parameters where assumed to be high and assumed rigid.

Table A.1: Report of the tests from Volvo Cars. [19]

Direction	Behavior	Maximum sliding/rotation	Stiffness/Force
x	Friction	$\pm 1\ mm$	Sliding at 60 N
y	Rigid	0	-
z	Rigid	0	-
Rotation around x	Rigid	0	-
Rotation around y	Linear elastic	$\pm 0.17\ rad$	1150 Nmm/rad
Rotation around z	Rigid	0	-

B   Properties with different materials

The tested parameters with different material combinations are presented in this appendix. The properties are close to the ones with the standard material combination.
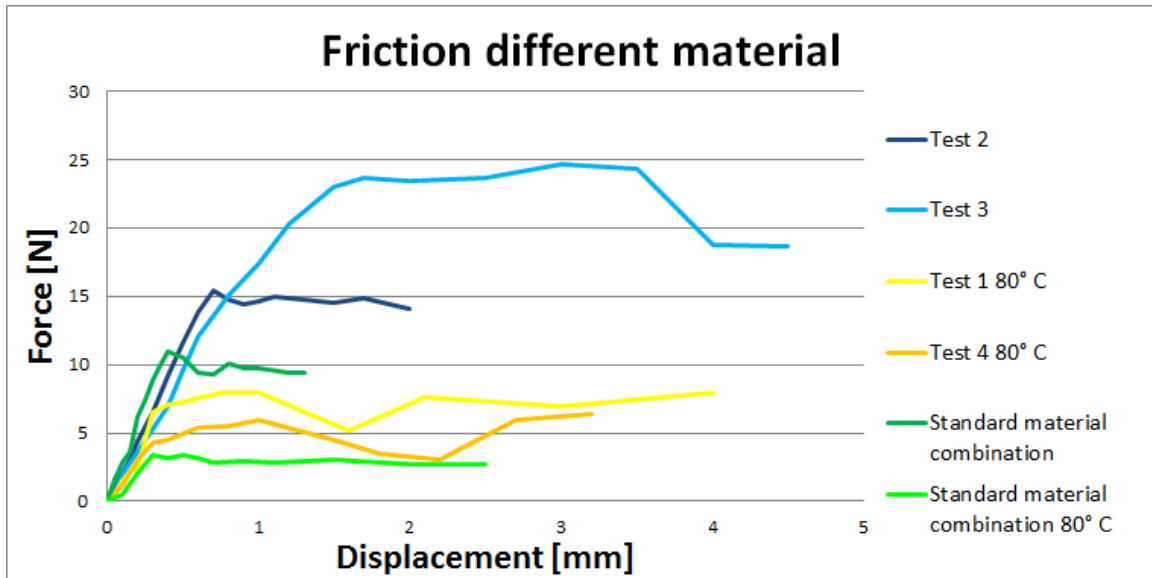

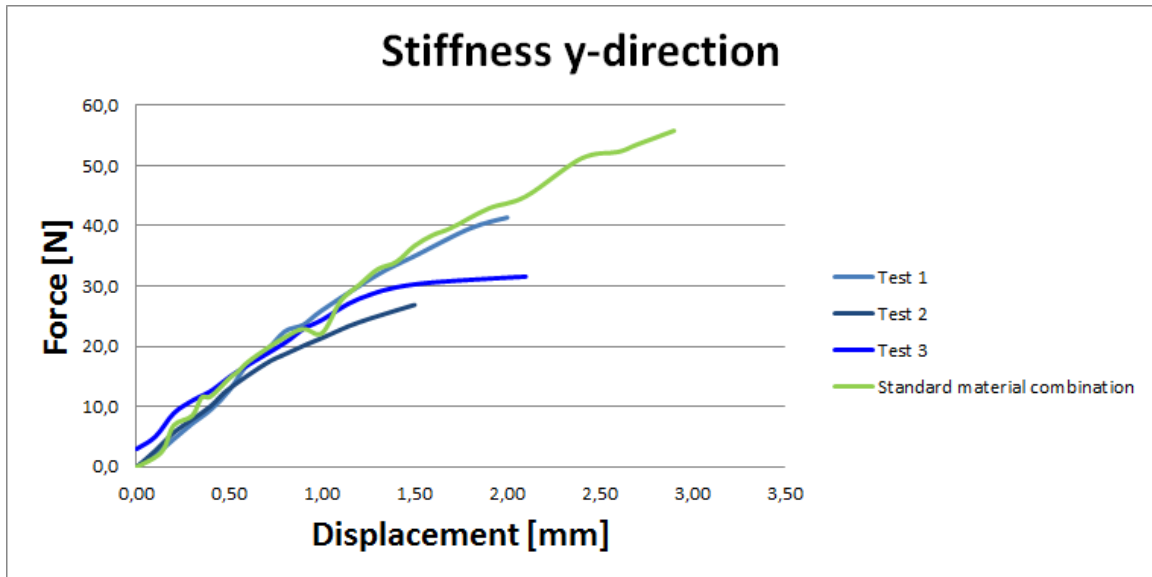Figure B.1: *Friction tests with different material combination.*

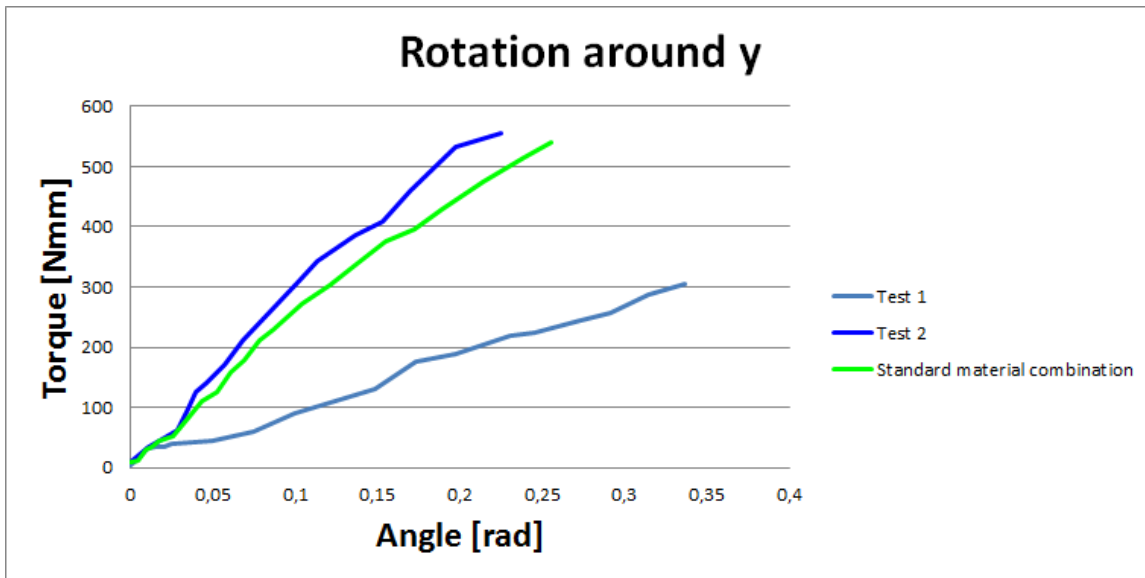Figure B.2: *Force vs displacement tests in y direction with different material combination at room temperature.*

Figure B.3: *The required torque vs the applied angle around the y axis with different material combination at room temperature.*
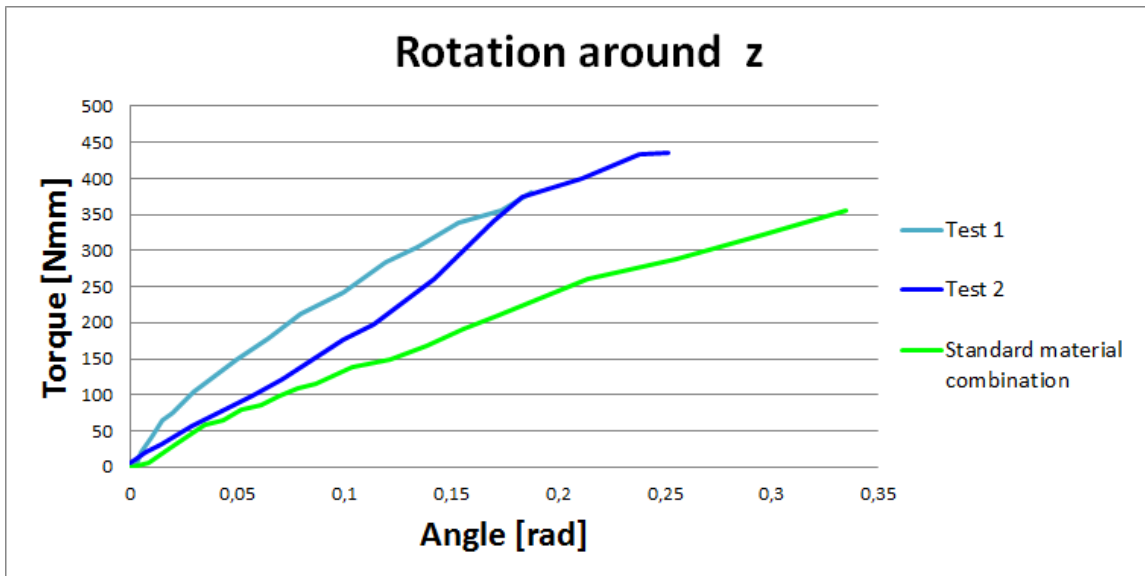

Figure B.4: *The required torque vs the applied angle around the z axis with different material combination at room temperature.*

C   Different dis-assembly variants

In the simulation of the dis-assembly process is different loadings possible. Here is a simple investigation of the difference in result between drag and push as loading case done. With drag is meant that the displacement loading is on the base of the tower as used in this report. The push is instead to apply the loading at the top of the clip. The result of the different loadings is shown in Figure C.1 and Figure C.2. The difference is approximately 20% but it is in the margin of error from other parameters in the analysis.
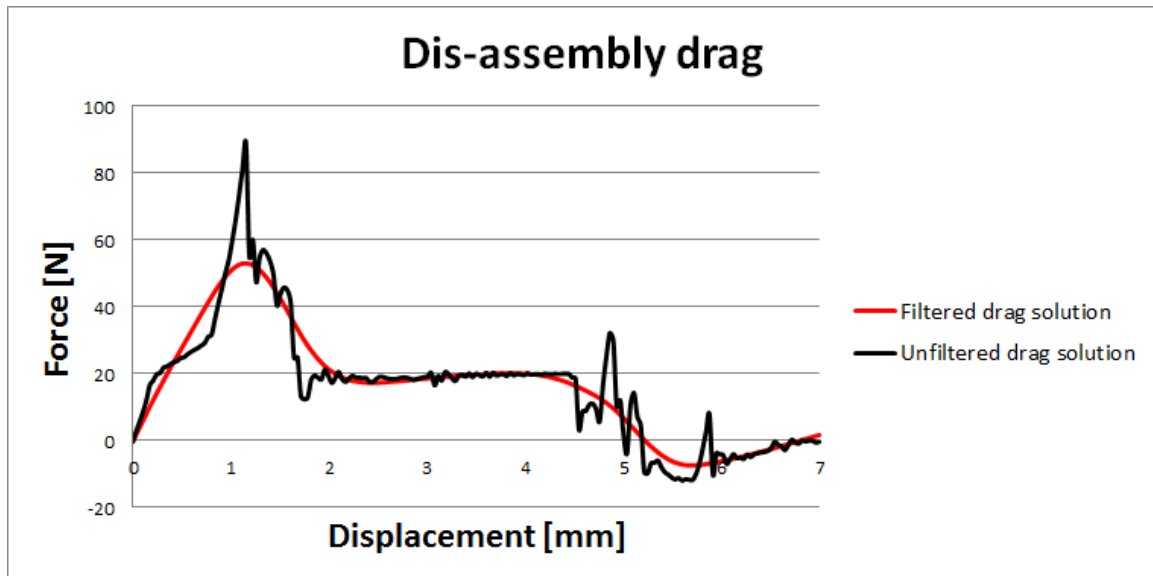

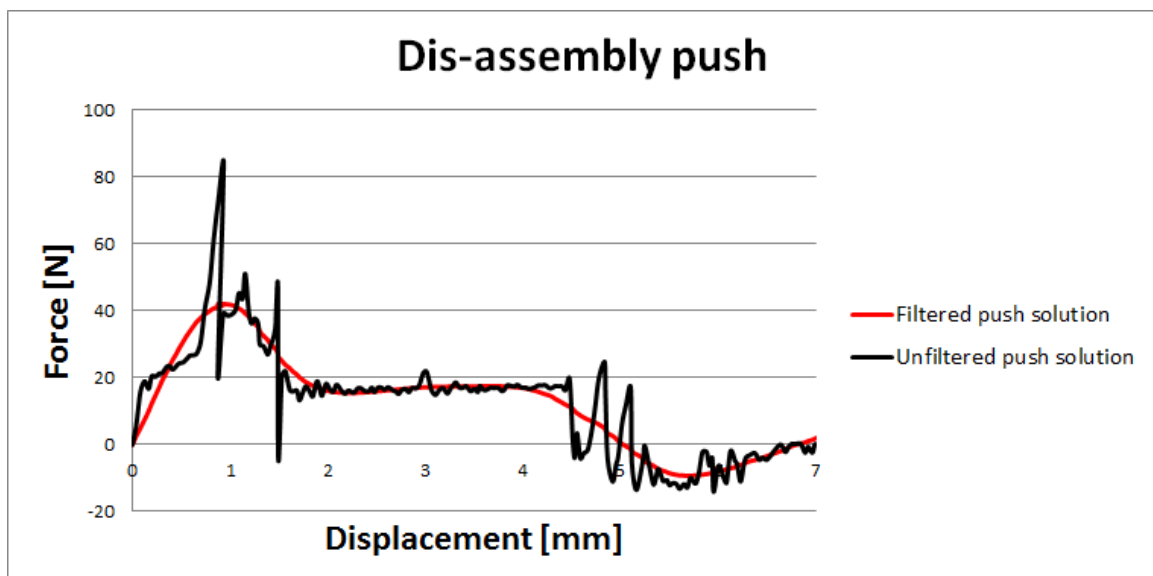Figure C.1: *Dis-assembly process with drag loading.*

Figure C.2: *Dis-assembly process with push loading.*

D   Numerical problems in contact and friction

Here is the problem in the dis-assembly simulation with a clip thickness 0.45 mm in the sensitivity analysis presented. The problem is based on the contact and friction model. In Figure D.1 is the red and blue curves the used friction and the green and purple is the same simulation but excluding the friction.

The simulation with friction gives a value of the dis-assembly force that is too high and not realistic. From looking at the simulation can be concluded that the reason for the high value is that the parts get stuck in each other. When doing the simulation without the friction is the parts not stuck together in the same way. So the problem is from the contact and friction model.

In Figure D.1 can be seen that the maximum value with and without friction is not at the same displacement. This is not expected due to that the maximum force in reality is probably at the same displacement and the magnitude is only changing with different frictions.
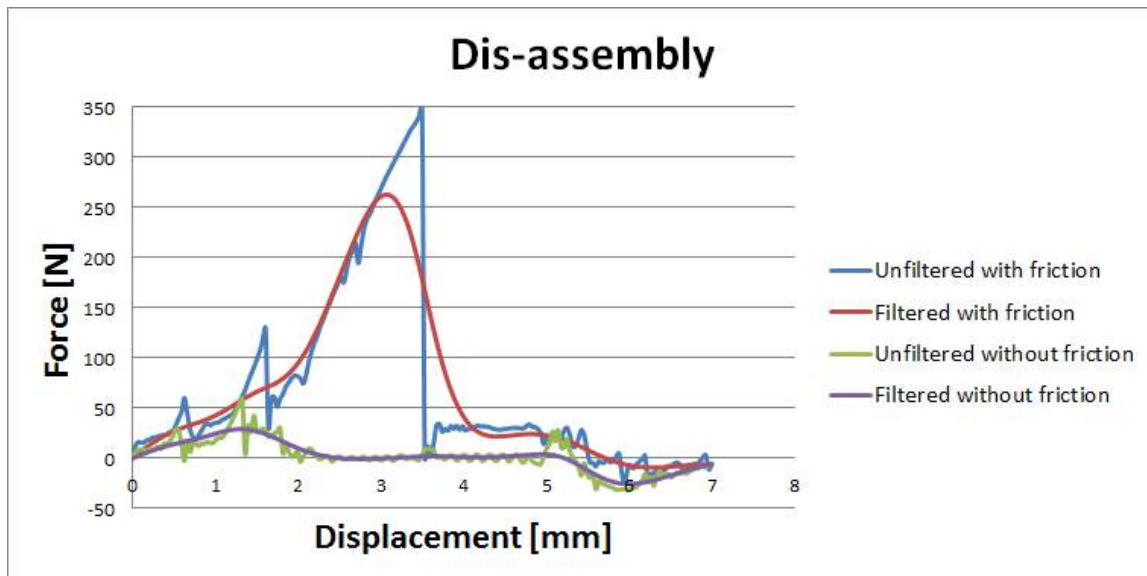

Figure D.1: *Simulation with problem with and without friction.*

D.1 Energy investigation of numerical problem

In Figure D.2 is the reaction force in one of the dis-assembly simulations that have numerical problems shown. Together with this is the different non zero energies also shown.
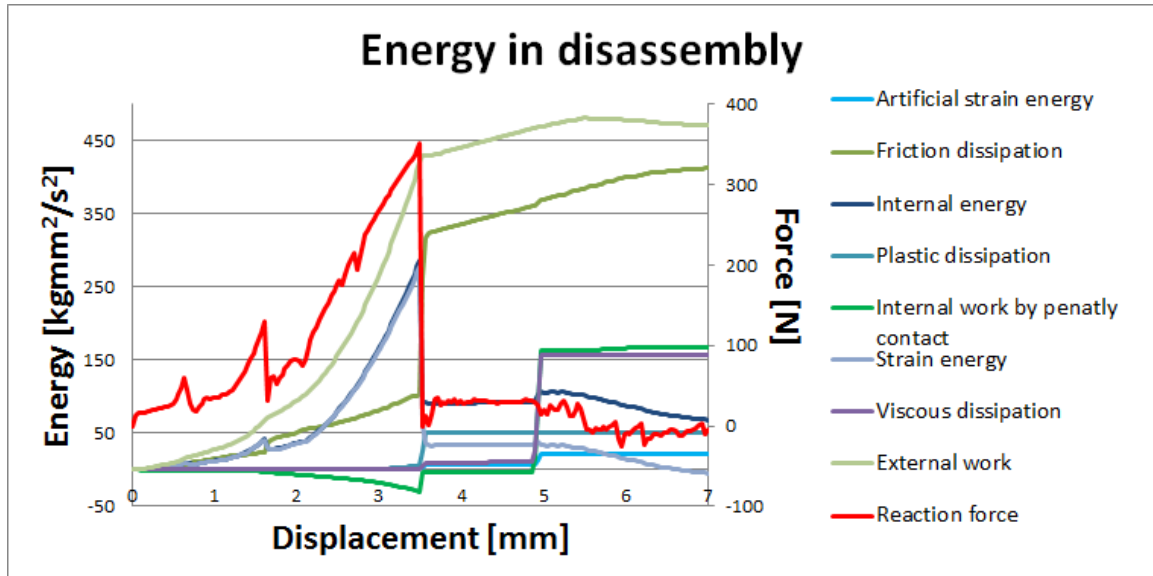

Figure D.2: *Energy changes in clip joint under dis-assembly for simulation with numerical problem.*

E   Energy investigation

In this part are the energies under the different loadings shown for the nominal simulation. In the following parts is also the behavior behind the energies discussed.

Under the assembly of the clip on the tower is only external work needed to overcome the frictional dissipation, see Figure E.1. When the flanges starts to entering the hole is the internal energy build up as strain energy in the clip. Exactly when the flanges come in to the hole is a lot of energy transformed from work by the penalty contact to viscous dissipation. This is probably due to something numerical but does not affect the solution.

Figure E.2 shows the change in energies under loading the clip with friction in x-direction. In the stiffness region is the clip deformed and the energy is stored in the clip. When sliding then occur is all the applied energy transformed to heat from the frictional dissipation.

In Figure E.3 is the energies under the loading for stiffness in y-direction presented. Under the loading is the most part of the external energy used to deform the clip and is stored as strain energy in the clip. Some energy is also needed to overcome the friction but it is approximately one third of the applied energy.

The energies under the rotational loading around the y-axis is shown in Figure E.4. In the loading is it in the first part only needed to add energy to deform the clip. This energy is saved as strain energy in the clip. In the next part is friction also needed to overcome and this energy is dissipating. In the last part is the loading not trustful and therefore is this not looked at.

In Figure E.5 is the force and the energies in the rotation around the z axis presented. The applied energy is transformed to strain energy and heat from the friction. Before the friction is fully developed in sliding in all parts of the contact is it builds up in two rounds.

In Figure E.6 where the dis-assembly process is shown can be seen that the frictional dissipation is increasing under the hole process but it matches that there is friction through the hole process. The strain energy is build up in the beginning of the loading until and released when the flanges has passed the hole. When the flanges passes the hole is also other energy released that was build up in the assembly process.
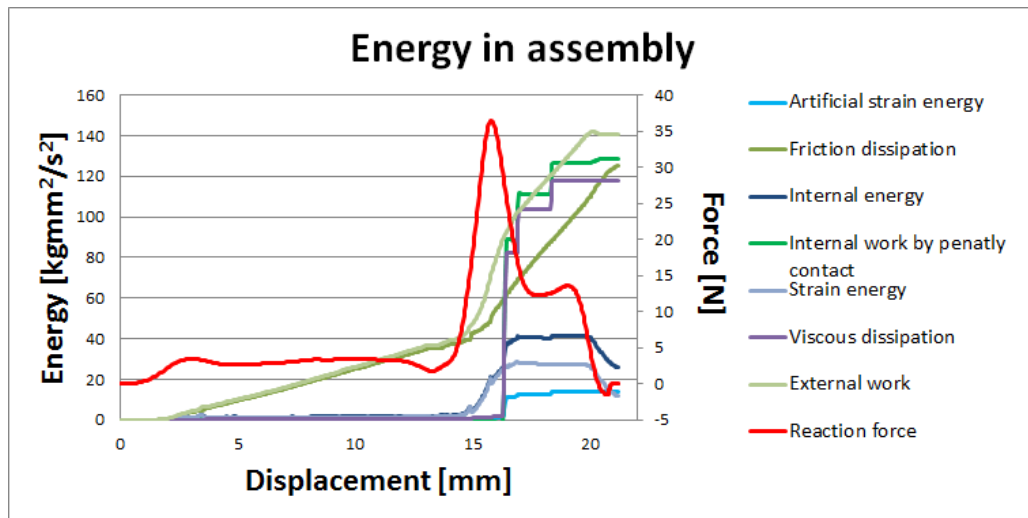
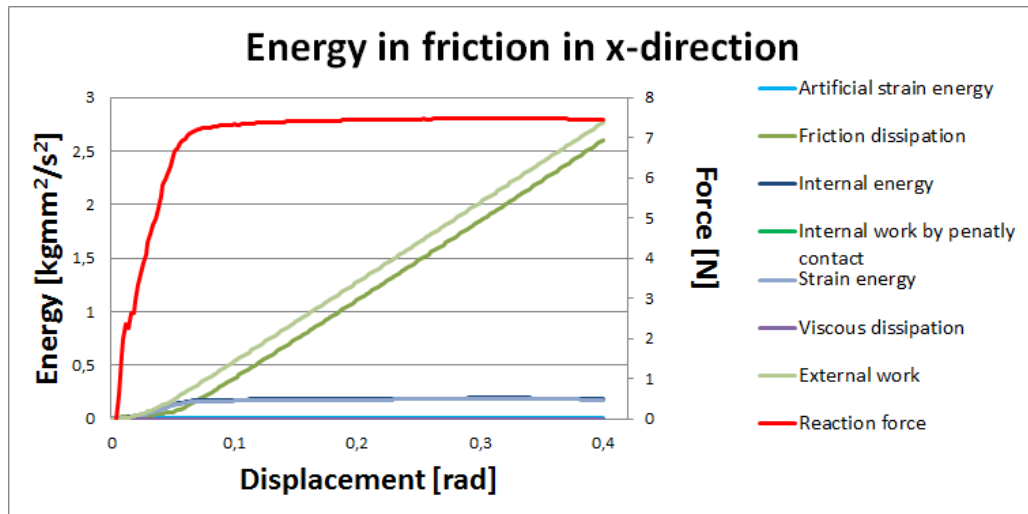Figure E.1: *Energy changes in clip joint under assembly for nominal simulation.*

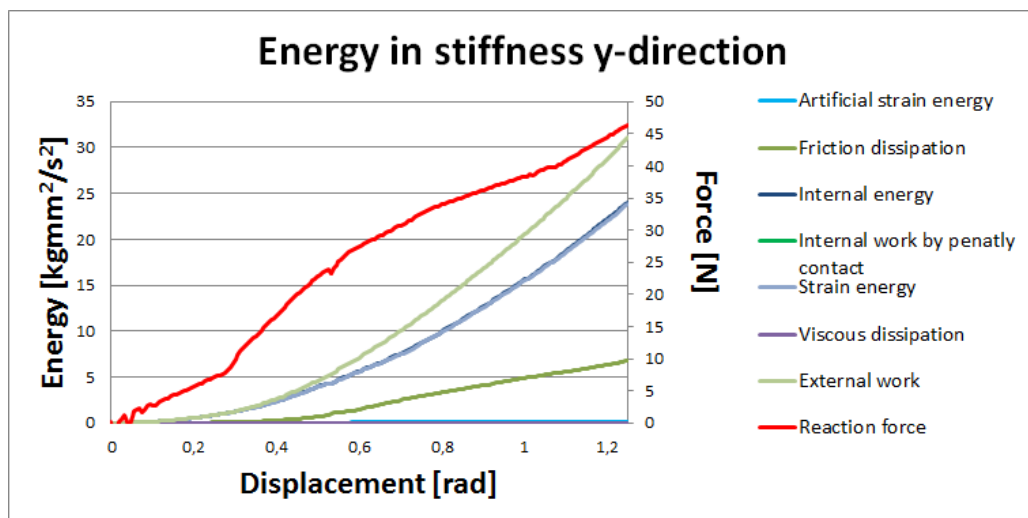Figure E.2: *Energy changes in clip joint under friction for nominal simulation.*

Figure E.3: *Energy changes in clip joint under loading i y-direction for nominal simulation.*
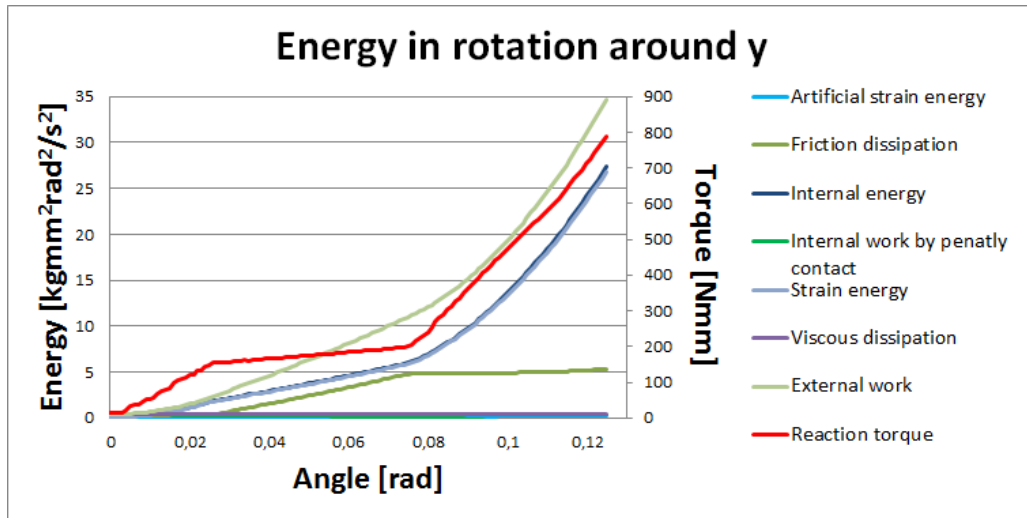
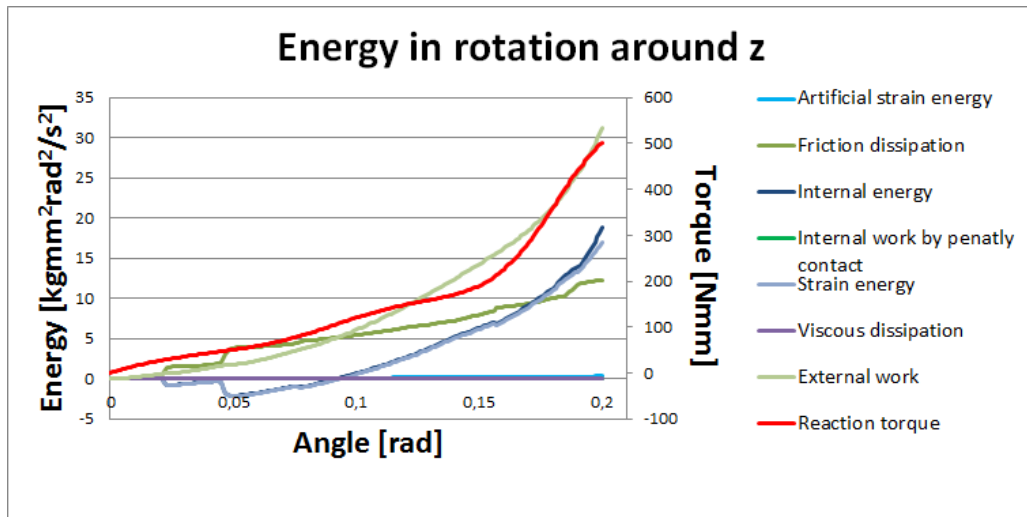Figure E.4: *Energy changes in clip joint under loading around y-axis for nominal simulation.*

Figure E.5: *Energy changes in clip joint under loading around z-axis for nominal simulation.*
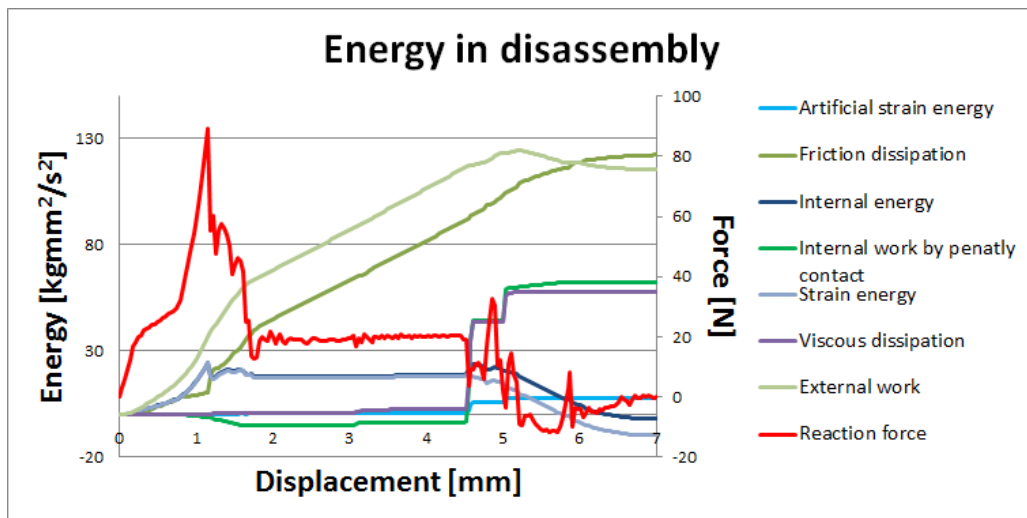

Figure E.6: *Energy changes in clip joint under dis-assembly for nominal simulation.*

F   Check of rotation around x

To get a clue of the rotational stiffness around the x-axis even if it is not included in this study is one simulation done with the nominal model. The simulation is shown in Figure F.1. In this can clearly be seen that there is a change in stiffness at approximately 0.075 rad. The stiffness in the first part is approximately 4000 Nmm/rad and in the second part 11500 Nmm/rad. The second part is not used due to the high value.
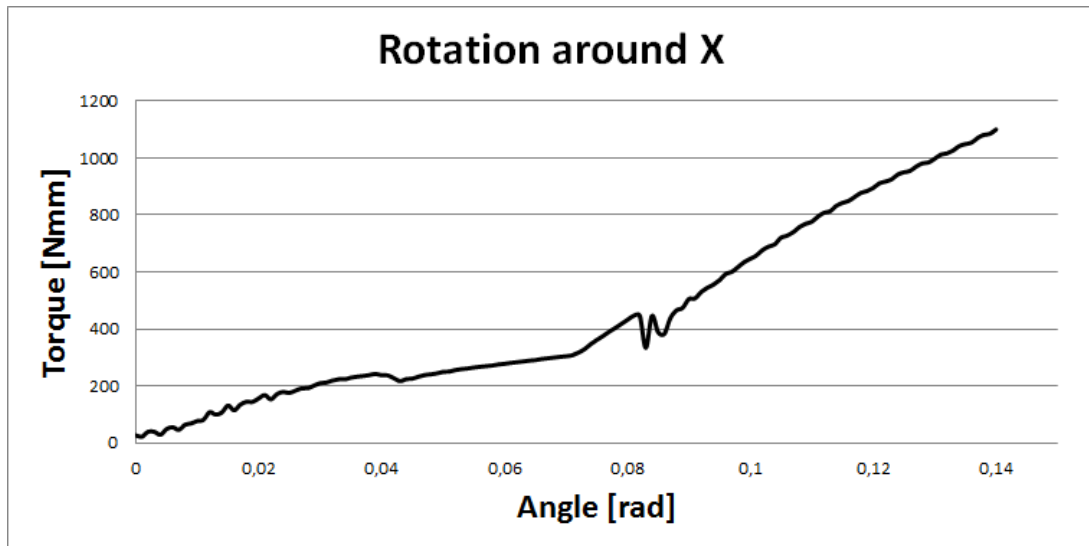

Figure F.1: *Simple simulation to get a clue of the rotational stiffness around x.*

G   Sensitivity analysis values

In Table G.1 is the values from the sensitivity analysis presented. The values are not exact and can vary depending on at between witch points the stiffnesses are calculated.

Table G.1: The variation of the values in the parameter variation.

	Assembly [N]	Dis-assembly stiffness [N/mm]	Dis-assembly force [N]	Stick stiffness [N/mm]	Friction [N]	Stiffness y [N/mm]	Rotational stiffness y [Nmm/rad]	Rotational stiffness z [Nmm/rad]	Simulation time [min]
Nominal (843 element on clip, hole = 8.5 mm)	36,4	52,3	53,1	128,3	7,3	38,4	3087,0	1264,0	158
Changed E +10% (231 GPa)	41,8	38,5	57,4	123,7	7,0	34,0	3525,0	1473,0	180
Changed E −10% (189 GPa)	32,3	30,6	46,4	102,2	5,8	27,8	2688,0	1200,0	164
Fine mesh on clip (1621 elements)	42,3	33,6	Numerical problem	148,1	6,2	29,5	1705,0	1333,0	229
Friction coefficient hole +20% ($\mu = 0.36$)	39,0	39,7	68,8	104,2	7,9	31,1	3925,0	1470,0	169
Friction coefficient hole −20% ($\mu = 0.24$)	33,5	29,3	40,9	112,3	5,0	31,0	2400,0	1230,0	172
Friction coefficient tower −16,7% ($\mu = 0.3$)	35,9	32,7	51,4	120,9	6,3	29,9	3562,0	1310,0	172
Friction coefficient tower +16,7% ($\mu = 0.42$)	36,8	34,6	52,0	121,8	6,4	32,2	3056,0	1382,0	170
Hole size +5,9% (9 mm)	23,0	23,7	33,4	110,0	3,8	25,2	1025,0	589,0	171
Hole size +11,8% (9.5 mm)	13,8	10,9	17,4	73,2	1,6	19,7	750,0	125,0	171
Hole size −5,9% (8 mm)	50,4	77,9	126,0	155,6	11,9	44,4	4362,0	1837,0	172
Moved clip on tower (+1 mm)	38,0	32,3	49,7	107,2	6,6	30,6	3050,0	1400,0	176
Moved clip and tower (+1 mm of clip) (+1 mm on tower)	36,5	33,1	49,8	124,5	6,6	30,5	1683,0	1315,0	180
Full integrated elements	36,3	33,4	53,9	130,0	6,7	32,2	3325,0	1350,0	288
Clip thickness +12,5% (0.45 mm)	54,5	41,8	Numerical problem	166,0	8,7	41,8	3716,0	1874,0	162
Clip thickness -12,5% (0.35 mm)	23,6	21,6	35,1	107,6	4,4	21,2	1731,0	879,0	172
Temperature increase (80°C)	-	52,0	53,1	141,5	7,5	38,3	3087	1255,0	110
Long time	39,3	33,3	55,6	151,5	6,3	31	3087	1283,0	371